Institut Polytechnique des Sciences Avancées (IPSA)

Aerospace Engineering

Final Thesis Project

Hybrid engines on passenger aircraft

Author: Antonio Montero Barriga

Tutor: Remi Bertossi

Co-Tutor: Luis Miguel García-Cuevas González

July 9, 2021

Abstract

This paper highlights the benefits of hybrid aircraft architectures over combustion aircraft and performs a state of the art on the current electric batteries technology. Furthermore, a new initial sizing methodology for hybrid aircraft is defined. It will be based on the analysis of the constraint diagram followed by an energy based iterative process for the determination of the MTOM. This innovative methodology is not based on Breguet's range equations since electric batteries are not a consumable source of energy. Furthermore, this hybrid sizing process will be applied to the Cirrus SR-22 aircraft to show the performance difference between a conventional and a hybrid-parallel propulsion systems. The results obtained show that for smaller mission ranges and cruise speeds than the original Cirrus SR-22 mission, substantial fuel savings are achieved. Nevertheless, this will increase the wing loading and power-to-weight ratio of the aircraft, shifting its design point upwards and to the right.

Nomenclature

Symbol	Definition	Units
AR	Aspect ratio	-
BSFC	Brake Specific Fuel Consumption	kg/(W·s)
c	Consumable	-
C_D	Drag coefficient	-
$C_{D,0}$	Zero lift drag coefficient	-
C_L	Lift coefficient	-
CVT	Continuously Variable Transmission	-
ddp	Deep discharge protection	-
DoH	Degree of Hybridization	-
e	Oswald factor	-
E	Energy	J
E^*_{bat}	Battery specific energy	W·s/kg
EM	Electric Motor	-
FEA	Full Electric Aircraft	-
g	Gravity constant	m/s^2
H_E	Degree of Hybridization of energy	-
H_P	Degree of Hybridization of power	-
HEA	Hybrid Electric Aircraft	-
ICE	Internal Combustion Engine	-
k	Induced drag factor	-
L/D	Lift to drag ratio	-
m	Aircraft current mass	kg
m_{bat}	Battery mass	kg
m_e	Empty mass	kg
m_f	Fuel mass	kg
m_p	Payload mass	kg
MTOM	Maximum Take Off Mass	kg

nc	Non consumable	-
NoD	Number of propulsion devices	-
P	Power	W
P/W	Power-to-Weight ratio	-
PH	Parallel hybrid	-
q	Dynamic pressure	Pa
R	Mission range	m
RoC	Rate of climb	m/s
S	Wing surface	m^2
S_G	Ground run distance	m
SH	Serial hybrid	-
T/W	Thrust-to-Weight ratio	-
tf	Trapped fuel fraction	-
TLAR	Top-Level Aircraft Requirement	-
TO	Take-off	-
U	Cruise speed	m/s
v	Speed	m/s
W/S	Wing loading	-
$\Delta m_{f,EM}$	Battery mas required for a given time step	kg
$\Delta m_{f,ICE}$	Fuel mass required for a given time step	kg
Δt	Time step	s
	Minimum error for iterative process	-
η_p	Propeller efficiency	-
η_{StT}	efficiency chain, from shaft-to-thrust	-
η_{BtT}	efficiency chain, battery-to-thrust	-
μ	Ground friction coefficient	-
λ_{bat}	Battery strategy parameter	-
ρ	Air density	kg/m^3

Contents

1 | Introduction

Over the last decades, the aviation industry has been growing very rapidly due to the increase in worlds'economy which makes transport aviation more accessible. However, this fact added to the increase in ground transport has resulted in an excessive growth of fossil fuels energy consumption. As it is already known, fossil fuel combustion has considerably negative effects on the atmosphere and Earth's environment.

Consequently, this has motivated the world's concern on climate change. Since several years, many researchers and industries have raised great efforts to find a solution and reduce the adverse effects produced by fossil fuels consumption. One of the most relevant efforts is the NASA N+3 project which aims to reduce the fuel consumption on the aeronautic industry by a 70% by the year 2025 [1], N+3 stands for the 3 future aircraft generations. The main objective is to reduce the CO_2 and the other polluting emissions due to fuel combustion. Another example is the goals set by ACARE in the project European flightpath's 2050 goals which involves reducing CO_2 emissions per passenger kilometer by a 75%, a 90% in NO_x emissions and a 65% in noise; with respect to the values of year 2000. [2].

To fulfill such an ambitious challenge, the aviation sector has already implemented several solutions like the progressive introduction of fuel cells and battery powered vehicles for ground operations at airports; or the improvement of fuel engines to increase its efficiency. However, these improvements are not enough to meet these targets. The implementation of electric propulsion systems is required to reduce the carbon footprint in the atmosphere originated by the aviation sector.

Electric propelled aircraft appear to be one of the most promising solutions. Its only drawback is the restriction imposed by the actual battery technologies which do not provide long flight time operations for a medium sized aircraft. The solution for the present time may rely on the intermediate point, hybrid propulsion.

This paper aims to determine the several hybrid propulsion system architectures for aircraft and to build conclusions on an initial sizing algorithm for such an aircraft. Firstly, a full definition of an Hybrid Electric Aircraft (HEA) will be performed with the advantages and disadvantages of each configuration against conventional aircraft designs. Secondly, a state of the art on the batteries will be carried to show in which level is the current technology and which are the possible ways of evolution.

Next, an initial sizing algorithm for hybrid aircraft will be defined taking as a basis the conventional aircraft sizing process. Furthermore, the results obtained with this procedure

will be analysed for its optimum design point with regards to the minimum MTOM. Finally, with the purpose of improving the previous results, a battery utilization strategy will be characterised to show how electric batteries can be oversized to a certain extent to gain substantial benefits on fuel consumption without increasing too much the aircraft weight.

2 | Hybrid Electric Aircraft (HEA)

This chapter will focus on defining a Hybrid Electric Aircraft (HEA) and to give the main parameters which must be taken into account in its design. Furthermore, a deeper analysis comparing its advantages and drawbacks against a conventional combustion aircraft will be performed. Finally the different architectures of hybrid propulsion system will be analysed and compared.

2.1 What is a Hybrid Electric Aircraft

A Hybrid Electric Aircraft (HEA) is powered by two types of engines: a conventional combustion engine which is powered by fuel and an electric engine powered by electric energy stored in a battery. These aircraft benefit from the reduction in CO_2, noise and other contaminant emissions to the atmosphere thanks to the production of electric energy. Compared to conventional propelled aircraft, HEA have a lower range as the energy density of, for example, lithium-ion batteries is much lower than fuel. Nevertheless, the efficiency of the electric engine is superior to the one of a conventional motor allowing to reduce the fuel consumed [3] [4].

Usually, both types of engines are working at the same time to generate the required power and reduce the pollutant emissions from the internal combustion engine. Commonly, HEA use the gas turbine engines to drive electrical generators to power the electrical motor driven fans. However, depending on the aircraft type and the flight mission considered, thrust may be provided via a combination of gas turbines and electrical propellers, or only by the electrical propellers. The several possible approaches will be detailed in section 2.2, along with the state of the art of batteries technology developed later in section 3.

Hybrid engines are no longer a new technology, they have been used since many years in several industries such as automotive vehicles, marine and trains. They have proved to offer some advantages over conventional engines such as:

- Improved efficiency and reduced price of the energy/fuel required.
- Use of excess power to supply auxiliary systems.
- Easier maintenance since electric engines have less mechanical components.

- No pollutant emissions and reduced vibration and noise.

2.1.1 Advantages over conventional engines

First and foremost, the most relevant benefit associated to HEA is the reduction in polluting and greenhouse gases thanks to the inclusion of electric engines. Another significant benefit is the flexibility in configuration and operation for the different flight phases. Depending on the duration of the flight, the electric batteries can be used for specific moments of the flight in which more power is demanded or used continuously throughout for shorter flights.

However, to efficiently take profit of these advantages of HEA, there exist some significant challenges for its design process. First of all, the weight is the most limiting parameter for any aircraft, so its overall efficiency will be decreased with the increase in weight. The main drawback of employing electric engines is their lower power density compared with conventional ICE engines, particularly at high power levels. Therefore, the addition of electrical engines must be capable of outcoming the negative effects of the extra weight of batteries and more with the gains in efficiency and reductions in noise and fuel consumption HEA designs [5].

Compared to a FEA (Full Electric Aircraft), HEA propulsion also inherently adds losses to the system through the intermediate use of electrical and combustive power. The efficiency of the electrical-mechanical power conversion and distribution processes, will suppose a source of energy losses on the system to a certain extent. Nevertheless, due to the current state of the art of batteries technologies it is prohibitively heavy to size a full electric propulsion system for medium and large aircraft, it is mostly used in drones or unmanned UAV as it will be seen later [6]. It is also important to mention that HEA are also restricted to a great extent by the technology development of electric components. However, its design is currently more feasible and profitable than the one of FEA. In chapter 3 a deeper analysis of the current and incoming technology in the future will be done.

2.2 Powertrain configuration

As already stated, a hybrid propulsion system is composed of at least 2 types of engines. Nevertheless, there are several configurations that allow to combine them in such a way that the aircraft efficiency is maximised depending on its mission requirements. In a HEA there are 2 energy storage systems: fuel for the ICE, which is a consumable source of energy; and electricity for the electric engine which is stored in a battery, this is a weight that will not be consumed over time. For the fuel/battery hybridization system, there appear 3 main configurations: series, parallel and series-parallel [4] [7].

2.2.1 Series configuration

In a **series** hybrid configuration, the propeller engine is only driven by the electric motor (EM) [8]. The main characteristic of this configuration is that the engine does not contribute to thrust generation [4]. Hence, it operates as a turbo-generator which thanks to the cyclic motion of the turbine of the combustion engine will produce electric power. This electricity will be used to charge the on-board battery, which at the same time will feed the electric propeller and the rest of on-board systems. In the following figure, a simplified scheme of this architecture is observed:

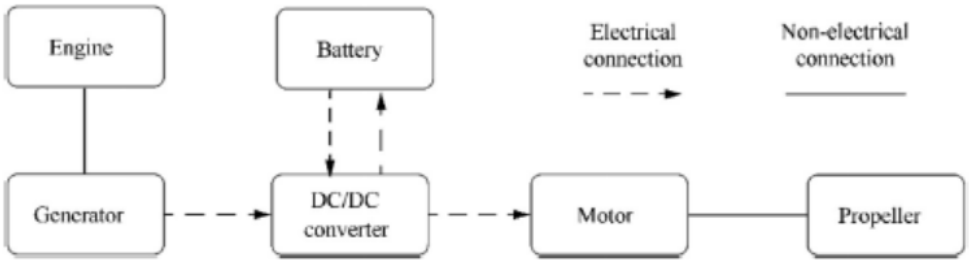

Figure 2.1. Series configuration [8]

The main benefit of the series hybrid configuration is having the conventional engine decoupled from the propeller. As a result, the engine can run at its optimal operating rate at any time regardless of the power demanded by the propeller depending on the flight regime. This will allow to maintain a lower fuel consumption since the ICE will be operating at its maximum efficiency. Moreover, as the combustion engine has no mechanical links with the EM, there will be a certain flexibility to place it along the aircraft. This can be used to benefit for a better air-intake position or to balance the center of gravity of the aircraft.

However, this configuration has a major drawback. The conversion of the mechanical energy generated at the ICE turbine to electric energy has a poor efficiency. Due to its massive power losses during the energy conversion, the series configuration is not so used for long flights.

Furthermore, as shown in figure 2.1 this configuration makes use of 3 components: combustion engine, generator and electric motor. This means that all of them need to be designed, sized and maintained periodically; increasing the cost and weight of the hybrid system significantly. Last but not least, having the ICE engine decoupled from the powertrain does not allow to reach a maximum overall power as the one that would provide the sum of the combustion and electric engines operating at the same time.

The series hybrid electric system is the most easily integrated system due to the versatility provided by its mechanical decoupling. Accordingly, it is widely accepted as the alternative propulsion system to hybridize multi rotor aircraft like drones and large scale airplanes.

2.2.2 Parallel configuration

In a **parallel** hybrid configuration, both the combustion engine and the electrical motor drive the propeller via a mechanical link, so they can contribute to the propulsion energy either simultaneously or individually [8]. In addition, the ICE does not only drive the propeller but also drives the electric motor/generator simultaneously, charging the batteries of the EM. As shown in Figure 2.2, other advantage of the parallel over the series configuration is that the number of components is reduced. The parallel configuration has the generator integrated within the electric motor. Also, a smaller engine and a smaller electric motor can be used to provide the same performance.

Another advantage is that only one of the two sources of power, mainly the ICE, must be sized for the highest sustained power at climb phase; as it exists the possibility of using both engines at the same time when more power is required. Since there will be two engines driving the propeller separately, the propulsion system will be safer than with series architecture due to engine redundancy. In case of failure it is possible to land with the electric engine without major hazards. Finally, since there is no conversion from mechanical to electrical energy, the power losses are also reduced in comparison with the series configuration.

Regarding its drawbacks, having the combustion engine mechanically linked to the propeller imposes a constraint on its optimum rotational speed. This happens because the rotational speed that the propeller will have at some phases may not be the optimum for the ICE. To solve this problem a Continuously Variable Transmission (CVT) can be implemented to allow the independence of the engine's and propeller's rotational speed. Nevertheless, there is a more economical approach which consists in developing an energy management strategy. Despite it requires a complex design process, this strategy can optimize the power contribution of the engine and the motor, which enables the propulsion devices to operate at their respective optimum conditions [8]. This approach will be detailed in chapter 7.

Parallel hybrid propulsion systems are further classified according to the position of the electric motor/generator in the drivetrain. Firstly, if the fuel engine is connected to the motor/generator but not directly linked to the propeller, the architecture is called **single-shaft** since the transmission has only one input shaft, this is shown in Figure 2.2. As commented before, in this architecture, the speed of the components of the system is always rigidly linked to that of the propeller. However, mid-scale hybrid airplanes prefer this option since it has a reduction in weight due to its mechanical simplicity, improving the propulsion system's efficiency as a result.

On the other hand, if the ICE and the EM/generator are mounted on two separate drive shafts, as depicted in Figure 2.3, it is called **double-shaft** parallel configuration. Having two separate shafts makes possible that the speed of the ICE and the EM are different from the propeller since each one have its own shaft. Therefore, the ICE can operate at its optimum speed.

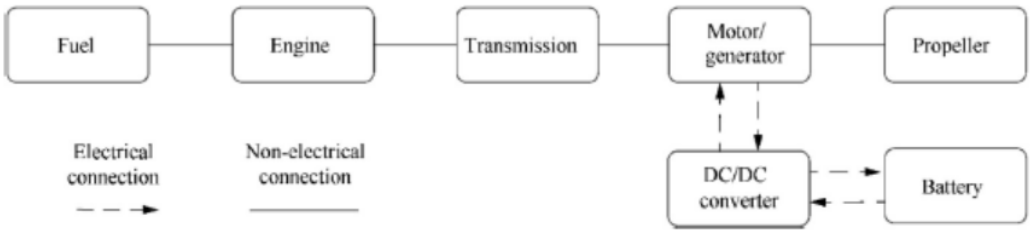

Figure 2.2. Single shaft parallel configuration [8]

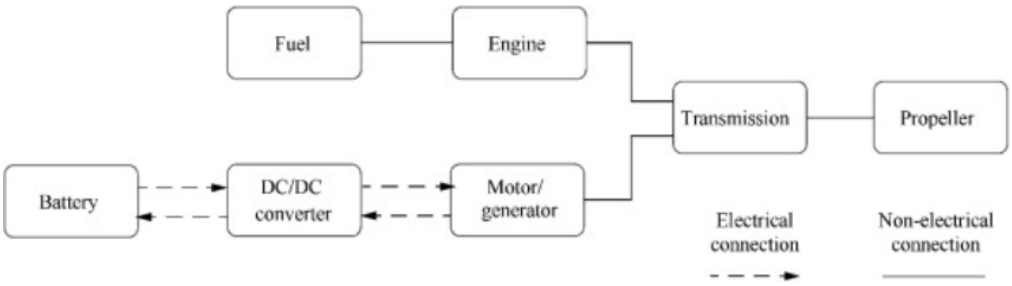

Figure 2.3. Double shaft parallel configuration [8]

2.2.3 Series-parallel configuration

As it can be imagined from its name, the **series–parallel** configuration, also recognized as power-split configuration, is a mixture of the two previous architectures. On this case, the three devices (ICE, EM and generator) are connected to a planetary transmission gear.

The advantages of this configuration comprise: a more flexible power distribution since it is possible to use the engine and the battery to power the propeller at the same time. This will allow the engine and the motor to operate in its most efficient region. However, this structure requires the most complicated clutch/gearing mechanism and energy management design.

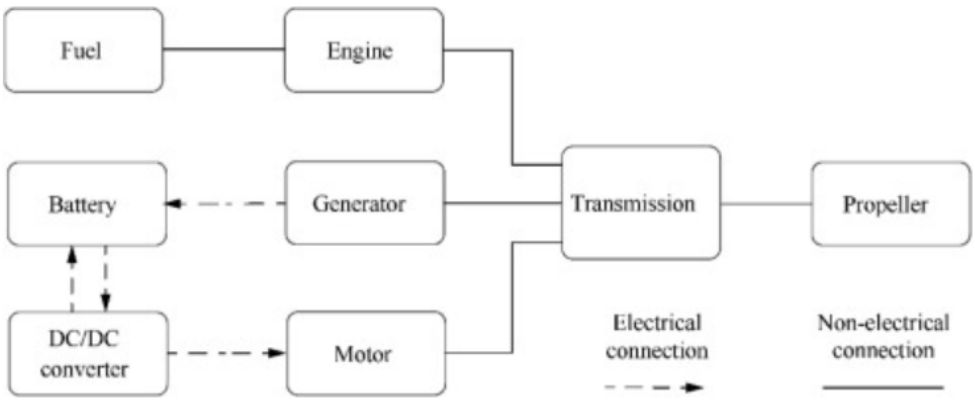

Figure 2.4. Series-parallel configuration [8]

2.2.4 Non-hybrid electric configurations

Although this report is focused on HEA, a brief description of the full electric and turbo-electric architectures will be performed. To show that there are other solutions to the fuel consumption reduction problem exposed in the introduction.

Pure electric architecture

The FEA aircraft is powered by a set of electric batteries connected to a EM. As a result the capabilities of these type of aircraft will be highly dependent on the current technology of electric batteries and electric motors. The main advantage of FEA is the reduction of fuel contaminant emissions and the increase of efficiency on energy conversion.

However, this is not a fully environmentally friendly propulsion system. It is important to control and analyse the source of production of the electric energy that will be used to charge the batteries. If it is generated with pollutant energy sources, there will still exist a damage to the environment associated to the FEA. In addition, when the life cycle of the batteries comes to its end it is important to carefully recycle and manage its waste. All of this is also extrapolated to HEA design.

The principal restrictive issue for FEA is the current available technology on electric batteries and motors. Until 2035 there are not expected significant changes on its performance which can mean a great economic improvement for commercial aircraft [9] [10]. As a result, its actual application is limited to short range aircraft such as UAVs, ultralight aircraft and eVTOL [6] [9].

Turbo-electric architecture

In turbo-electric configurations, the single energy source is a gas turbine. Therefore the aircraft does not use batteries to store the energy. This supposes a great benefit since its performance will not be restricted to the technology barrier of electric components as it happened for hybrid and full electric configurations [9].

For a full turbo-electric configuration, all the energy generated by the gas turbine will be transformed into electric energy and used to move one or several EM connected to the propulsive device. On the partial turbo-electric architecture, the gas turbines are also connected to the propeller and the excess of energy is used to move the EM. As it can be seen, it is really similar to the series-parallel configuration with the difference that no batteries are used.

The disadvantage of turbo-electric propulsion systems is that fuel emissions are not reduced to a great extent since the electricity is being generated in its totality by the gas turbine. However, a reduction in fuel consumption is achieved in comparison with conventional aircraft. This is due to the higher energy efficiency of EM and the reduction in weight coming from the elimination of the batteries.

2.2.5 Architecture of study

To sum up, on this chapter the most commonly used hybrid engine configurations have been analysed. The **series configuration** enables the engine to operate at its ideal rating in exchange of losing some efficiency due to the conversion of electric into mechanic energy. Next, the **parallel structure** allows for a simpler and lighter propulsion system. However, the rotational speed of the engine will be limited to the propeller one. Finally, the **series–parallel** is the most functional, but complicated configuration out of the three architectures. It is the least popular configuration concerning aircraft application due to its high complexity [8].

Because in the aeronautic sector weight reduction and redundancy are a critical factor for its design, the parallel configuration will be analysed with more detail in this report. As well as that, the parallel configuration benefits from a greater versatility level when talking about power distribution between the EM and the ICE. Even though, the parallel architecture has been determined the most profitable, there are not enough studies to show that this is the best choice. This will depend on the mission of the aircraft of study [10].

3 | State of the art of batteries

In this chapter, the state of the art of electric batteries will be developed to show the current technology level and the constraints to which FEA and HEA are attached to. The main problems rely on issues related with energetic and power density, weight and performance.

An electric aircraft is powered by electric batteries which provide a far greater chain efficiency in comparison to conventional propulsion systems. In addition, as stated in section 2.1.1, they benefit from an environmentally friendly operation, less maintenance operations and the fact that the gravity center does not move due to fuel reduction.

Nevertheless, electric technologies are not yet fully implemented on the aviation sector since the current technology gives a low autonomy and flight range. Its main drawback is the weight of the power source, which does not decrease over time.

3.1 Batteries

As it has been commented in the previous chapters, it results obvious that the main limitation to commercialise electric aircraft is the batteries development. Since 2015 or before, many research centers have been working to improve the capabilities of electric batteries, mainly focused on ground applications.

Contrary to the development followed by terrestrial electric transport industry, the aviation sector has a huge constraint for its design: Weight. Nowadays, the specific energy of batteries is enough to make electric cars and other ground vehicles a direct competitor to its conventional fuel models. However, the specific energy is not yet high enough to design HEA which provide a similar performance to conventional ones. Only small aircraft such as UAVs and ultralight aircraft are being properly hybridized. Even in the case of these relatively small airplanes in which it is possible to take off, the weight of the batteries limits the payload, reduces its autonomy and, therefore, restricts its use.

Clearly, the battery performance is not the only criteria to do not fully commercialise electric or hybrid aircraft. There are other disadvantages related to the battery application.

- **Overheating of the batteries**. This will imply that a corresponding cooling

system is required for its safe operation, thus increasing the overall weight.

- **Instability**. As many experiments has demonstrated, the theoretical predictions for this technology does not always match the real performance. Therefore, it is a very dangerous and unpredictable system, which is a crucial point for safely transporting civilians.
- **Autonomy and charging time**. The energy supplied by the batteries is really limited. Also, the charging time of the batteries may be a difficulty during the sizing of every flight phase.
- **Battery waste**. Once the batteries have finished their life cycle, its recycling process must be controlled since they are really contaminant.

Next, the three more promising battery technologies in development will be exposed together with their theoretical and practical energetic densities. The objective of this is just to show the current state of the art of the energetic density provided by its model, which is the parameter which mostly constraints the HEA design. Consequently, the internal chemical process which allows the batteries to store and release electric energy will not be analysed.

3.1.1 Lithium - Ion (Li-Ion)

Nowadays, the Li-Ion family of batteries is widely used in the industry due to its high energetic density. They have been already used in several hybrid aircraft projects of big enterprises such as the hybrid aircraft Boeing 787 Dreamliner or the EFan-X of Airbus [11].

According to several research performed on this technology, the actual energetic density is over 250 Wh/kg. Therefore, even though Li-Ion batteries are a mature and already tested technology, its energetic density is not yet high enough to fully develop HEA without too many design constraints. However the following paper [12] states that each year Li-Ion batteries designs are improved and its energetic density will grow a 6%.

3.1.2 Lithium - Sulfur (Li-S)

Recent studies executed on this technology has shown that they will be able to reach energetic densities of about 470 Wh/kg, Oxis Energy [13]. In addition, Oxis Energy expects an improvement on its technologies, being able to design prototypes of 600 Wh/kg in the near future.

This values are greater than the ones shown for Li-Ion batteries. However, Li-S batteries have a big drawback. Its life is more limited than in the case of Li-Ion and the economic investment on Li-S batteries will be greater, making it unprofitable for commercialization. This is due to uneven current densities on the anode surface which cause lithium to coat

and shed unevenly when the battery is charged and discharged many times. This will reduce the available surface of the anode and therefore decrease its performance.

More research is required to increase its life time and specific energy to outcome the economic difference with respect to Li-Ion batteries.

3.1.3 Lithium - Air (Li-Air)

This technology is pretty new and it is already in development. They use oxygen as oxidiser and as a result its weight is reduced considerably. This property provides a theoretical energetic density about 10 kWh/kg, this is several orders over the previous technologies. However, there only exist theoretical studies by the moment and it is obvious that in practice its performance will be lower.

As already stated, these batteries are not fully developed yet so there is a big discrepancy and uncertainty in the theoretical values obtained from several investigations. Some examples of the research studies on Li-Air batteries are: Kaushik Rajashekara 2000-3500 Wh/kg [14], S.Stückl 750-2000 Wh/kg [15], or Lonnie Johnson 5200 Wh/kg [16]. Therefore, this high discrepancy in the results manifests the uncertainty of the development of Li-Air batteries. This means that this new technology needs several years before becoming a more promising and practical electric source to be implemented.

3.2 Extracted conclusions

After having reviewed the most interesting battery technologies for electric or hybrid aircraft applications, we can determine that Li-Ion batteries are the most operational option by the moment. Its high use and maturity in the industrial sector is a big advantage when assessing production costs. Nevertheless, in the near future Li-Ion batteries could be replaced by Li-S; provided that its life time is enlarged. Regarding Li-air batteries, this can be the best solution for the electrification of aircraft on the long term. However, there is still too much work to do to achieve a safe and precise operational prototype.

For the viability of a hybrid or electric aircraft to be possible, a battery energy density much higher than the current one is required. According to Boeing [17] and [18], the electrification of air jets will be an option to consider once the batteries exceed an energy density of 750 Wh/kg.

Beyond this threshold, it should be noted that batteries may have a high specific energy value but generally have low specific power values. For example, a battery may be capable of storing a lot of energy, but it is only capable of releasing it slowly, and therefore such a battery may be useful in an electric aircraft to provide autonomy, but not acceleration. Accordingly, on HEA batteries are not used when high power peaks are required because they are unable to supply fast energy.

This relationship between the specific energy and the specific power of a battery is a

very important aspect of technological performance that is usually represented graphically by means of a Ragone diagram, as can be seen in figure 3.1. This diagram clearly shows how after the specific energy threshold described (750 Wh/kg) starts to decrease for higher power densities.

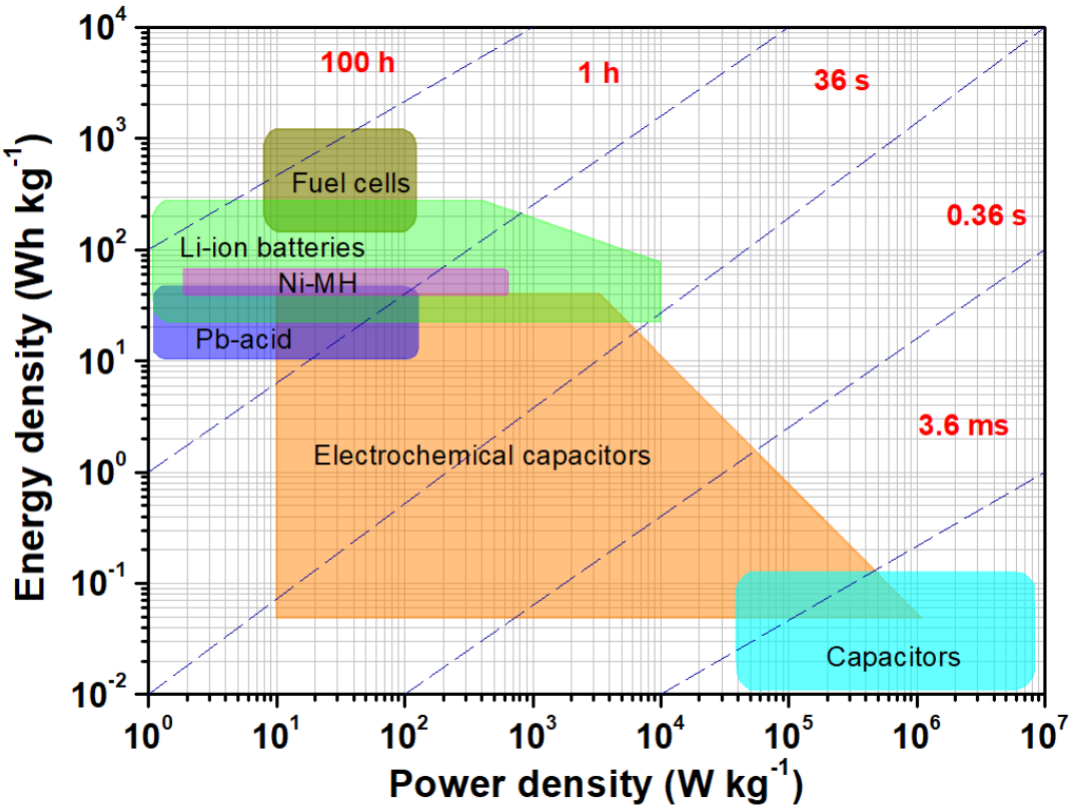

Figure 3.1. Ragone diagram [19]

In this section, the actual limit for the specific energy for batteries has been set about 250 Wh/kg. However, a great development is expected on the following decades. To assess how this evolution will affect the future HEA designs, on chapter 6 calculations will be done for the actual batteries of 250 Wh/kg and for a future value of 500 Wh/kg.

4 | Initial sizing process

After having clearly defined what are the main characteristics of an hybrid propulsion system and its main configurations, an aircraft conceptual design methodology will be defined. On this chapter, a review on the sizing process for conventional aircraft will be performed to easily define the hybrid sizing process in the following chapter.

4.1 Initial sizing

The first task to perform before anything is the initial sizing of the masses of the aircraft and the top-level aircraft requirements (TLARs). This first guess of the main aircraft parameters is performed without knowing the real design and geometry of the final model. However it will allow to perform a first design.

The main questions that designers must answer are:

- How heavy will the new aircraft be for the given set of requirements?
- How big will the engines be for the new design?
- Which wing area will be needed?
- Cost of this new design?

Since the cost is a magnitude which varies on several external non-physical parameters such as offer and demand of the different components in the market, to answer to the last question a figure of merit will be defined. Generally, designers chose aircraft's weight as the main cost design parameter [20] [21]. Therefore, the MTOM (Maximum Take Off Mass) will be used as a figure of merit in this study.

Focusing now on the other three questions, it is important to remark the influence of take-off weight, wing reference area and thrust on the initial sizing process. These parameters will be highly determinant for aerodynamics and structure calculations as well as for the propulsion system choice. Once a first guess of these parameters is performed and the power plant has been chosen, further refinement can be performed to obtain a more accurate weight and wing reference area for a new detailed sizing process.

4.2 Conventional sizing process

The conventional aircraft sizing process described herein will be the basis of the hybrid sizing process characterised in the next chapter.

The traditional sizing algorithm can be divided in two big parts: the point performance and the mission performance. The first one, **point performance**, allows to determine if a specific aircraft design will accomplish all point performance constraints for all the flight envelope. After the initial sizing, with the first guess of the MTOM parameters such as maximum thrust or maximum combustion power could be assessed as a function of T/W (Thrust-to-Weight ratio), P/W (Power-to-Weight ratio) and W/S (Wing or surface loading). Afterwards, the MTOM will be recalculated during the mission performance analysis through an iterative process. Secondly, the **mission performance** will be applied to estimate the MTOM of the new designed aircraft with the already known parameters T/W, P/W and W/S from the point performance analysis.

To correctly compute the MTOM of any aircraft, it is important to know all its components: Empty mass, fuel mass and payload mass.

$$MTOM = m_e + m_f + m_p \tag{4.1}$$

Since only the value of the payload mass is fixed and known before the design process and empty and fuel masses depend on MTOM, an iterative process must be carried starting with the initial guess of MTOM until reaching convergence with an error lower to ϵ. The following scheme clearly shows this iterative process concerning MTOM.

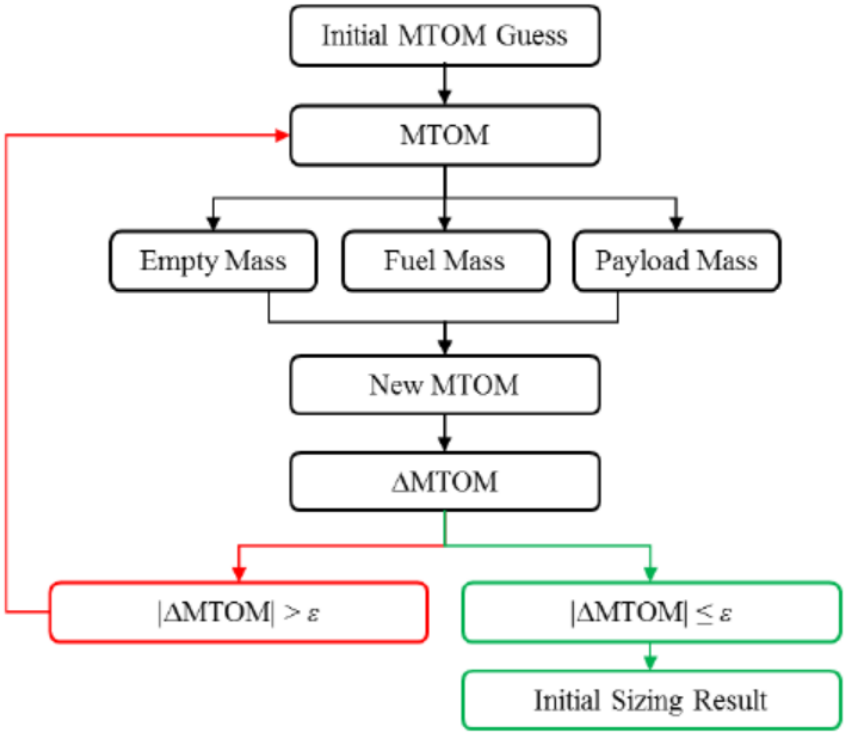

Figure 4.1. Mission performance sizing process [22]

5 | Hybrid sizing methodology

This chapter will fully develop the initial sizing process for hybrid aircraft. The scope will follow the two main steps from the conventional aircraft design procedure: Point performance and mission performance.

5.1 Hybrid sizing process

When applying the previous methodology for an hybrid aircraft there appears a big drawback for fuel mass computation. For conventional aircraft, the fuel mass always decreases with time. Nevertheless, this is not the case for hybrid aircraft which will use electric energy as part of their power source. Batteries will be a constant weight that the aircraft must be capable of carrying during all the flight. Therefore, the traditional equations for fuel mass estimation such as Breguet's range and endurance equations do not hold when an electric motor is introduced in the propulsion system.

A new methodology must be defined to asses hybrid aircraft sizing. Following the algorithms defined by Felix Finger [22] and Lucca Boggero [23] for hybrid electric aircraft and [24] for conventional aircraft; a new hybrid sizing process will be determined.

As shown in the following figure 5.1, the two main parts of the conventional scheme are kept: point and mission performance blocks.

Once the top-level aircraft requirements (TLARs) have been defined (how far, how fast, what payload the aircraft must carry...) through the initial sizing procedure described on section 4.1, the sizing process can begin. The input parameters required will be the first guess of MTOM and all the TLARs defined for the specific chosen aircraft.

After that, the point performance will be calculated through a matching diagram to assess the optimal design point (P/W and W/S) of the aircraft of study. Then, the mission performance analysis to determine the MTOM will be performed. This second analysis consists on an iterative process as defined in several classical aircraft design books [25] [26].

The complete methodology will be explained step by step in the further sections along with the required equations for its computation.

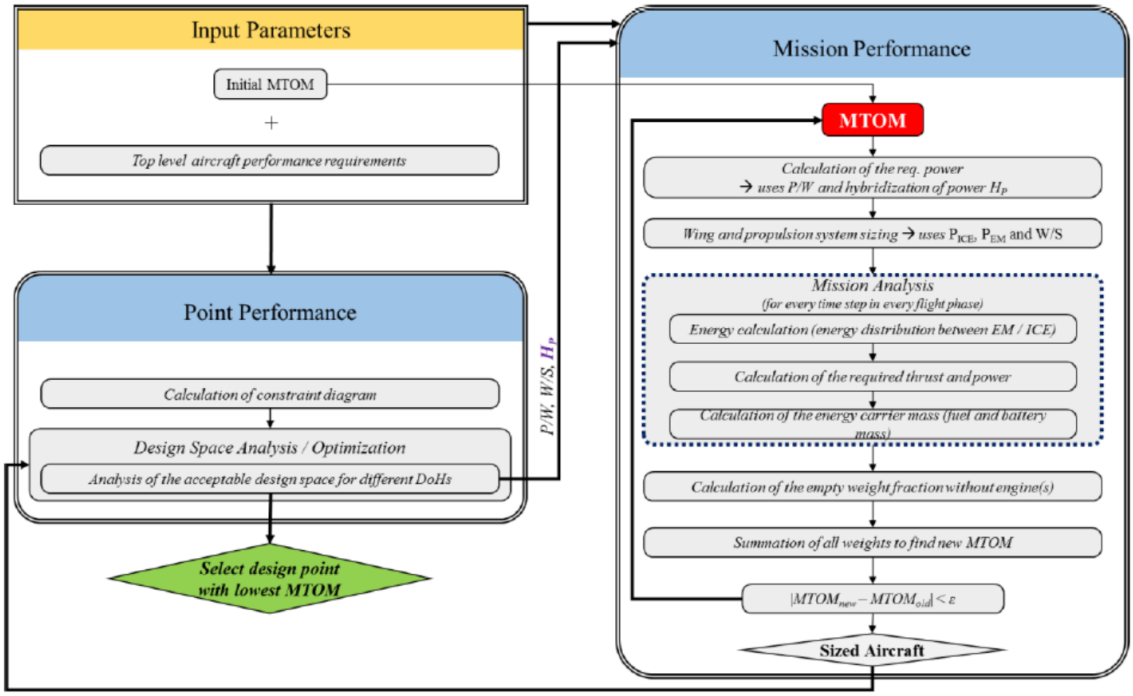

Figure 5.1. Hybrid sizing process [22]

5.2 Point performance

The point performance analysis is based on the matching or constraint diagram which is given by the intersection of 4 different curves. This graph will allow to see which power-to-weight ratio (P/W) corresponds to a given wing-loading (W/S). The constraint curves are the required take-off distance, cruise speed, rate of climb and the stall line constraint. These are the most basic and limiting design constraints, nevertheless it is possible to refine the process by adding more variables such as turn rate or service ceiling requirements.

In the following figure, the classical matching diagram can be observed. The crossing of all the constraint lines will give the design line which will divide the space between the acceptable and unacceptable region. As their names indicate, in the first one the P/W and W/S conditions established by all 4 requirements are met. Whereas in the unacceptable region, the thrust-to-weight (T/W) or power ratio (P/W) is lower than the constraints prescribe.

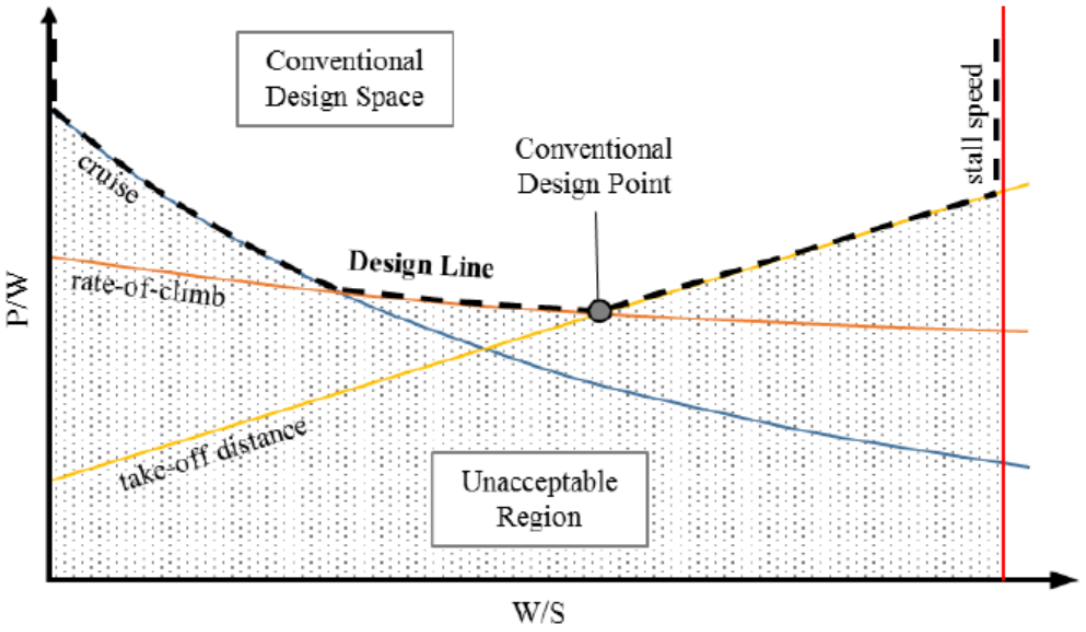

Figure 5.2. Conventional constraint diagram [22]

For the conventional approach, the design point will correspond to the lowest value of P/W and W/S from the design line. This point will give the option with the lowest mass which also grants the accomplishment of all the requirements. However, in the following sections this diagram will be used in a different way which is adapted for hybrid aircraft conditions.

5.2.1 Constraint equations

Thanks to the already defined TLARs several design parameters are fixed, now the W/S will become a design parameter. For each fight phase it exists a function of T/W depending on W/S. Therefore, this will give the required T/W in all flight phases.

The following constraint equations have been taken from [27] and extended with the advanced drag model from equations 5.1 and 5.2.

$$c_D = c_{D,min} + k \cdot (c_L - c_{L,0})^2 \tag{5.1}$$

$$k = \frac{1}{\pi \cdot AR \cdot e} \tag{5.2}$$

Before the evaluation of the constraint equations, some parameters of the aircraft will be defined. These relations have been extracted from [24].

$$v_{TO} = v_{stall} \cdot 1.1 \tag{5.3}$$

$$v_{climb} = v_{stall} \cdot 1.2 \tag{5.4}$$

$$C_{L,TO} = \frac{CL,max}{1.1^2} \tag{5.5}$$

Take-off distance constraint

This first constraint equation will determine the T/W required to achieve the desired ground run distance for take-off given by the defined TLARs.

$$\left(\frac{T}{W}\right)_{TO} = \frac{v_{TO}^2}{2 \cdot g \cdot s_G} + \frac{q \cdot c_{D,TO}}{\frac{W}{S}} + \mu \cdot \left(1 - \frac{q \cdot c_{L,TO}}{\frac{W}{S}}\right) \tag{5.6}$$

Applying the following relations this equation can be simplified:

$$v_{TO} = 1.1\sqrt{\frac{2 \cdot \frac{W}{S}}{\rho \cdot c_{L,TO}}} \tag{5.7}$$

$$q = \frac{\rho \cdot v_{TO}^2}{2} = 1.21 \cdot \frac{\frac{W}{S}}{c_{L,TO}} \longrightarrow \frac{q \cdot c_{L,TO}}{\frac{W}{S}} = 1.21 \tag{5.8}$$

$$\left(\frac{T}{W}\right)_{TO} = 1.21 \cdot \frac{\frac{W}{S}}{g \cdot s_G \cdot \rho \cdot c_{L,TO}} + 1.21 \cdot \frac{c_{D,TO}}{c_{L,TO}} - 0.21 \cdot \mu \tag{5.9}$$

Cruise speed constraint

This expression will give the required T/W to maintain the cruise speed at a certain cruise altitude. It must be taken into account that the dynamic pressure q will vary as the density decreases with altitude.

$$\left(\frac{T}{W}\right)_{cruise} = \frac{q}{\frac{W}{S}} \cdot \left(c_{D,min} + k \cdot \left(\frac{\frac{W}{S}}{q} - c_{L,0}\right)^2\right) \tag{5.10}$$

Rate of climb constraint

This expression will give the required T/W to necessary to achieve a desired rate of climb (RoC). This equation is an extension of the previous one, equation 5.10, but one must also take care about using the correct values of altitude and climb speed for the dynamic pressure.

$$\left(\frac{T}{W}\right)_{RoC} = \frac{RoC}{v_{climb}} + \frac{q}{\frac{W}{S}} \cdot \left(c_{D,min} + k \cdot \left(\frac{\frac{W}{S}}{q} - c_{L,0}\right)^2\right) \tag{5.11}$$

Stall speed constraint

This last constraint does not depend on the thrust-to-weight ratio and therefore it will just define a maximum value for the wing loading W/S. It corresponds to the vertical line

in the constraint diagram of figure 5.2.

$$\left(\frac{T}{W}\right)_{stall} = \frac{\rho}{2} \cdot v_{stall}^2 \cdot c_{L,max} \tag{5.12}$$

Conversion from T/W to P/W ratio

As it can be seen in figure 5.2, the vertical axis is given by the power-to-weight ratio P/W. Nevertheless, the constraint equations are defined for the thrust-to-weight ratio T/W. This is due to the fact that ICE and electric engines are rated in terms of power. Therefore, the following conversion equation will be applied with a propeller efficiency value of $\eta_P = 0.7$ [28] [29].

$$\frac{P}{W} = \frac{\frac{T}{W} \cdot v}{\eta_P} \tag{5.13}$$

5.2.2 Degree of hybridization - DoH

With all the constraint equations defined the matching diagram can be drawn. However, HEA have more degrees of freedom than conventional aircraft; this is what is called the degree of hybridization (DoH).

As defined in [22] a degree of hybridization will be defined for power and energy for both, parallel and serial architectures.

Degree of hybridization of power

This ratio, H_P, relates the installed propulsion power of the electric motors to the total installed propulsion power received by the propeller's shaft.

For parallel hybrid configuration the H_P is given by:

$$H_{P,PH} = \frac{P_{EM,max}}{P_{max}} \tag{5.14}$$

Nevertheless, for serial hybrid configuration this ratio will be always equal to 1 as all the power passes through the electric engine and the propeller is only driven by the EM. Therefore a new H_P for series configuration will be defined:

$$H_{P,SH} = \frac{P_{EM,max}}{P_{ICE,max}} \tag{5.15}$$

Degree of hybridization of energy

The second DoH will be the one of energy, H_E. It is defined as the ratio of the required energy delivered by the batteries, non consumable mass, to the total required transport

energy.

$$H_E = \frac{\Delta E_{nc}}{\Delta E} \tag{5.16}$$

This ratio is defined for every flight phase of a mission and determines the power request of EM and ICE in each phase.

5.2.3 Hybrid application of the constraint diagram

As explained in previous sections, the matching diagram will be used in a different way for the hybrid propulsion system sizing process.

In the conventional approach, the area below the design line was forbidden since at least one of the given constraints will not be met. Now, this region will be used to indicate the degree of hybridization in what is called the "P/W split space".

In the constraint diagram a design point will be defined, for hybrid aircraft this point is not necessarily the point with the lowest P/W and W/S. However, a point of the design line will still be selected since for a given P/W ratio the lowest MTOM will be given by the lowest possible wing loading. From now on, under this design point there will exist several "split points", which will indicate the power distribution between the ICE and the EM by means of the H_P hybridization factor. For each split point a complete new aircraft can be sized with a different H_P.

In the following figure 4 split points have been selected to show how this methodology works, all these points are related to the same design point

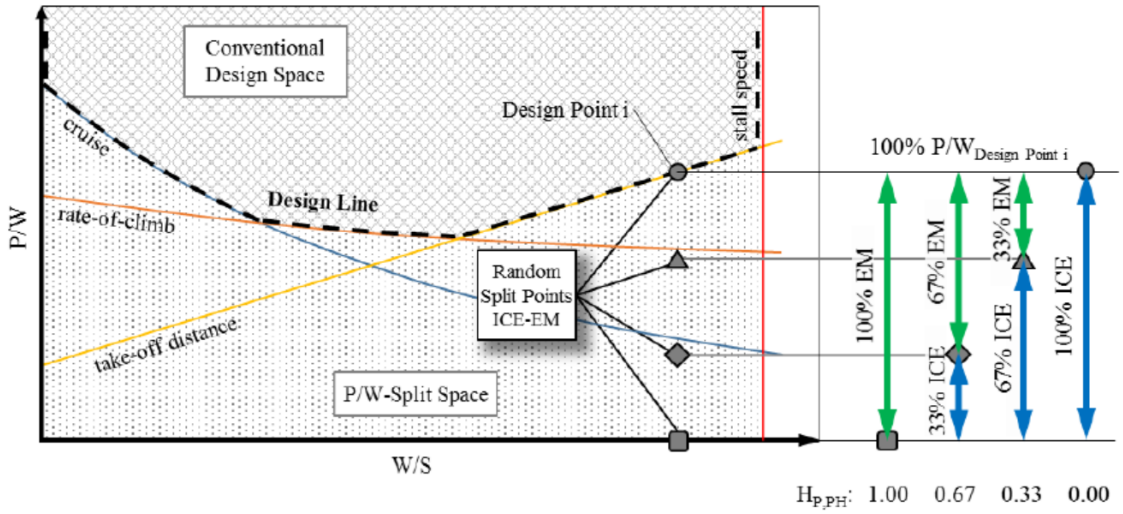

Figure 5.3. Parallel hybrid constraint diagram [22]

The first split point, the circle, corresponds to a conventional aircraft since it is located on the design line. It will use all the power from an ICE and therefore $H_{P,PH} = 0$. Secondly,

the triangle will correspond to a $H_{P,PH} = 0.33$ which means that 33% of the P/W is given by the EM and the other 67% left by the ICE. Nevertheless, it is important to remark that as this split point is located over the cruise constraint line, the ICE will be able to supply all the power required for this phase. For the diamond point, the opposite case to the triangle one is presented $H_{P,PH} = 0.67$. Finally the squared split point will be the case of a FEA with $H_{P,PH} = 1$. As it should be expected, the greater the hybridization degree the greater the size and weight of the required batteries to meet the aircraft requirements.

Although only the parallel architecture will be analysed, it has been found interesting to define the algorithm of use of the constraint diagram for the series architecture, which is slightly different. Since the propeller is driven by the EM at any time, the DoH of power as defined in equation 5.14 will be always equal to 1. This time the diagram will be used with the newly defined $H_{P,SH}$ for series configuration at equation 5.15.

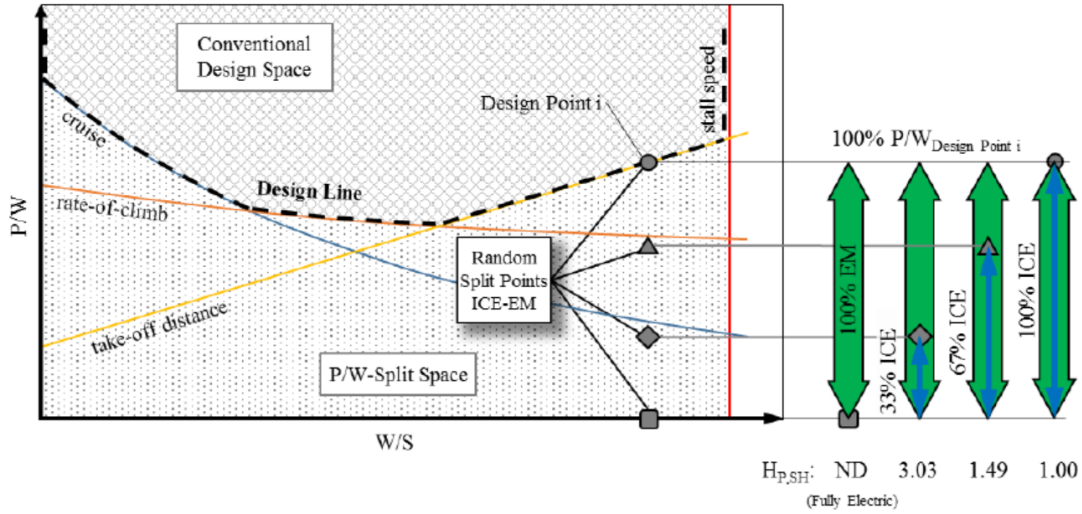

Figure 5.4. Series hybrid constraint diagram [22]

The only difference with the previous diagram is that the EM will always provide 100% of its output power and it is the ICE which will be reducing its contribution to the generation of electric energy.

The circle split point corresponds again to the case of a conventional propelled aircraft, $H_{P,SH} = 1$. For the triangle point, the ICE contribution will be reduced to a 67% and as a result batteries will be required to store electric energy, $H_{P,SH} = 1/0.67 = 1.49$. On this case, the aircraft would be able to fly on cruise without use of the energy stored in the batteries, the ICE is enough to drive the EM and the propeller. For the third case, the ICE contribution is reduced even more and greater batteries will be required, $H_{P,SH} = 1/0.33 = 3.03$. Again, the bottom point will correspond to a FEA with no contribution of the ICE, the $H_{P,SH}$ parameter is not defined since it will reach an infinite value.

5.3 Mission performance

Following the described diagram for the hybrid sizing process in figure 5.1, once the TLARs and the MTOM from the initial sizing process with the design P/W, W/S and H_P from the point performance have been defined, it is time to move to mission performance study.

The mission performance analysis uses the previous defined parameters as inputs to, thought an iterative process, determine the final MTOM of the aircraft. Since an HEA has two sources of energy, consumable (fuel) and non-consumable (batteries), the sizing algorithm will treat the masses as absolute values instead of as fractions. Moreover, Breguet's range and endurance equations do not hold for hybrid aircraft since the batteries do not reduce its mass with time. Instead, the mission is divided into short segments and simulated, using a universally valid, energy-based approach.

Some remarks on how works the iterative process must be provided to give a first understanding to the reader before entering into more detail.

- The mission is defined explicitly by TLARs defined at the initial sizing.
- Each flight phase is divided in small time steps Δt.
- Fuel and battery weight are determined from the energy required for each time step in which the flight phases are broken. The energy degree of hybridization, H_E will distinguish between consumable and non-consumable parts.
- After each time step of the iterative process, the consumable fuel mass is subtracted from the previous mass in the aircraft. The shorter the time step, the more precise the method.
- During the weight estimation process, based on the first estimate for the MTOM, the masses that make up the gross weight are calculated. From the point performance analysis the design P/W split point will allow to size the propulsion system and therefore determine its weight.

5.3.1 Propulsion system mass estimation and wing sizing

The first step will be to compute the maximum power required from the design P/W and the initial MTOM estimation. The DoH will give the amount of power supplied by the ICE and the EM.

$$P_{max} = \frac{P}{W} \cdot MTOM \tag{5.17}$$

Thanks to this preliminary calculation, an estimation on the weight and the power delivered by the ICE engine and the EM can be performed.

With the previously defined design point, it is also possible to obtain the wing reference area of the wings.

$$S = \frac{MTOM \cdot g}{\frac{W}{S}} \tag{5.18}$$

5.3.2 Energy sources mass estimation

For this step, the required power and energy for each flight phase will be computed, as well as the duration time of each phase. The following formula gives the required energy for each flight regime:

$$\Delta E = \frac{m \cdot g \cdot v}{\frac{L}{D}} \cdot \Delta t + \frac{m \cdot \Delta v^2}{2} + m \cdot g \cdot RoC \cdot \Delta t \tag{5.19}$$

In the previous equation, the first term accounts for the energy demand due to aerodynamic drag which applies for all phases. For acceleration phases the second term corresponding to the kinetic energy variation must be added. Finally, for climb and descend phases the change in potential energy, third term, will be added. In addition, during take-off the engine will be assumed to operate at maximum power.

Next, the transport energy will be separated between the consumable and non-consumable sources by means of the DoH of energy, H_E. With these data, the power required by each engine for every flight phase is computed. It is important to mention that not every flight phase will use the power from both sources.

$$\Delta E_c = \Delta E \cdot (1 - H_E) \longrightarrow P_{ICE} = \frac{\Delta E_c}{\eta_{StT,ICE} \cdot \Delta t \cdot NoD} \tag{5.20}$$

$$\Delta E_{nc} = \Delta E \cdot H_E \longrightarrow P_{EM} = \frac{\Delta E_{nc}}{\eta_{StT,EM} \cdot \Delta t \cdot NoD} \tag{5.21}$$

Finally, the required mass fuel according to the supplied power by the ICE for a given flight phase during a time Δt is:

$$\Delta m_{f,ICE} = (1 + tf) \cdot P_{ICE} \cdot NoD \cdot BSFC \cdot \Delta t \tag{5.22}$$

On the other hand, the required battery mass will be computed from the non-consumable required energy supplied by the EM.

$$\Delta m_{f,EM} = (1 + ddp) \cdot \frac{\Delta E_{nc}}{\eta_{BtT} \cdot E^*_{bat}} \tag{5.23}$$

Where tf stands for the additional trapped fuel fraction which will also contribute to the total mass. Whereas ddp stands for the percentage of deep discharge protection because if batteries are fully discharged they would be damaged.

Each flight phase will be broken into small time steps of 0.01 s or less. On every time step of the iterative process, the burned fuel mass will be subtracted from the overall mass.

Similarly, the required total transport energy, equation 5.19, should also be recalculated with the new mass at each time step. This process will give always a small error since the aircraft mass is changing at every instant, however $\Delta t = 0.01$ s is small enough to get an accurate result.

5.3.3 Empty mass estimation

The last mass which is left to determine is the empty mass of the aircraft. This is defined as the mass of all systems, structure and equipment without any payload and fuel. The ICE and EM that will be used will be sized later according to the required power-to-weight ratio. However, an initial empty mass estimation is also required on this step to start the iterative process. Higher order mass estimation methods can be used to get a more accurate result, but this is out of the scope of this paper.

5.3.4 MTOM estimation

With all the sub-masses calculated, now is possible to build the MTOM as the sum of all of them:

$$MTOM = m_e + m_f + m_{bat} + m_p \tag{5.24}$$

This new value of MTOM will be checked with the one of the previous iteration. If the difference between them is small enough, the iterative process will be stopped meaning that a convergent aircraft design has been reached for the given TLARs, design constraints and split point from the constraint diagram.

6 | Selected aircraft analysis

On this section a real aircraft will be submitted to the hybridization sizing process described in the last chapter. For doing so, the main parameters of a real aircraft will be defined as well as its TLARs for flight.

First of all a conventional baseline aircraft will be computed as a reference case to perform comparisons between the several hybrid solutions and the conventional solution. This will allow to analyse and assess the advantages or disadvantages of the parallel hybrid aircraft.

After that, several studies will be carried out with the same methodology by changing several design parameters to see how the different hybrid designs will behave. For each mission the split points will be selected with regard to the minimum MTOM. However, this will not be the most optimum design from the energy efficiency point of view, which will give a slightly higher MTOM. For the case studies, since some specific data was unavailable or difficult to access, the results obtained from the study [30], based on the previous initial hybrid sizing process, will be analysed and compared to determine which is the optimum configuration of parameters and for which type of mission.

6.1 Selected aircraft

The aircraft of study will be the Cirrus SR-22, it is a very well known aircraft on the aeronautic industry. This general aviation aircraft is propelled by a single IO-550-N propeller. The main aerodynamic parameters and TLARs of this aircraft have been kept as in the original model. This aircraft's data have been obtained from several sources [31] [32] [33].

As stated before, the designed aircraft will use a parallel hybrid propulsion system since its architecture allows to obtain a higher peak power by the addition of the contribution of both engines. Moreover, there will not be any loss from energy conversion as it happens in the series configuration and the propulsion system weight is reduced.

Table 6.1 shows the main geometric and aerodynamic parameters of the aircraft of study as well as the TLARs imposed by the mission. The flight will be a typical cruise mission, including 45 minutes of FAR dictated reserve energy. On table 6.2, the engine parameters used and its efficiencies are presented.

Mission requirements			**Aerodynamic parameters**	
m_p	380	kg	CL_{max}	2.111
U	90	m/s	CL_0	0.25
v_{stall}	32	m/s	CD_{min}	0.0254
RoC	5	m/s	L/D	0.866
S_g	340	m	AR	10.2
v_{TO}	38	m/s	e	0.7763
v_{climb}	41	m/s	k	0.0402
h_{climb}	3000	m	μ	0.03
Range	1150	km		

Table 6.1. TLARs for Cirrus SR-22

Engine parameters		
E-Motor Specific power	5	kW/kg
ICE Specific power	1.18	kW/kg
E^*_{bat}	250	Wh/kg
BSFC	314	g/(kW·h)

Table 6.2. Engine performance for Cirrus SR-22

6.1.1 Conventional baseline aircraft

As explained before, with the data given in tables 6.1 and 6.2 a first baseline case will be run to have relevant data to compare and evaluate the results obtained in the subsequent sections. The next table shows the obtained values:

	MTOM (kg)	W/S (N/m^2)	P/W (W/kg)	m_{fuel} (kg)	Energy (MJ)
Actual SR-22 data	1633	1152	141	-	-
Lowest MTOM	1558.8	1230	147.5	190.1	7691.8
Difference	-4.54%	6.77%	4.61%	-	-
Design point	1577.9	1136	132.1	223.4	9042.3
Difference	-3.37%	-1.39%	-6.31%	-	-

Table 6.3. Sizing results for Cirrus SR-22 conventional case

Two different sizing results have been shown. Firstly, the one which minimises the MTOM which has provided a MTOM of 1558.8 kg, slightly lower than the real Cirrus SR-22 (-4.54%). However, a higher wing loading and power ratio have been obtained. Secondly, the design point which is sized for the highest power loading has given a MTOM of 1577.9 (-3.37% difference) for a slightly lower P/W and W/S.

The results of the baseline case appear to be pretty accurate since the maximum difference is lower than a 5%. This is a low percentage for a initial sizing process which implies that the algorithm is accurate enough. Thanks to these results a comparison between the hybrid and conventional configurations will be performed in the following sections.

6.2 Point performance computation

Before moving to the hybrid aircraft sizing results it has been found interesting to show the constraint diagram for the baseline aircraft. Only this diagram will be illustrated since for every defined mission a new diagram will be labelled.

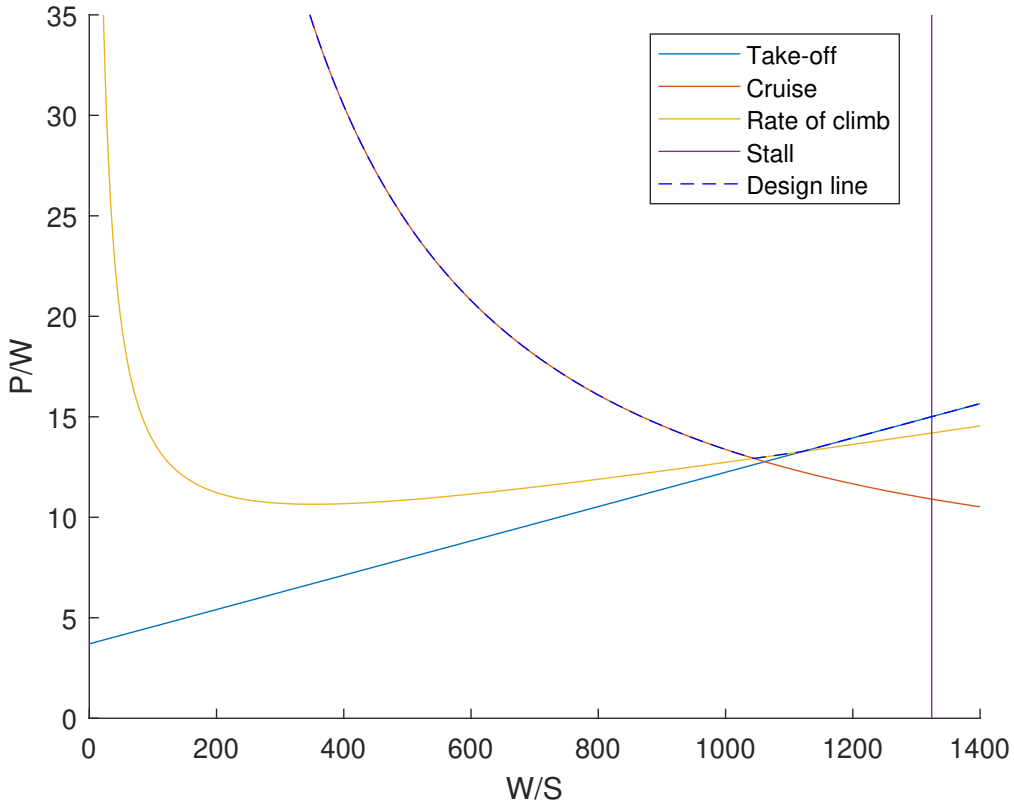

Figure 6.1. Constraint diagram

From the constraint diagram above, it can be seen that the phases which mostly constraint the mission are cruise for W/S below 1050 and take-off for W/S over 1100. It is important to remark the stall constraint line which is imposed for a wing loading of 1324. On the following analysis this will limit the complete use of the batteries' technology for several cases.

6.3 Hybrid sizing analysis

The parameters which will be changed to evaluate the performance and behaviour of the parallel hybrid aircraft design are the following:

- Altitude (3000 m - 1000 m)
- Battery specific energy (250 Wh/kg - 500 Wh/kg)
- Cruise speed (90 m/s - 75 m/s)

As a result $2^3 = 8$ distinct missions will be evaluated for each range and zero-lift drag coefficient (C_{D0}). In addition, the range and C_{D0} will be decreased from 1150 km to 575 km and from 0.0254 to 0.02 respectively. It is necessary to remark that, as stated in chapter 3, the current state of the art for batteries implies a huge constraint for hybrid and electric aircraft. With the aim of analysing how HEA will perform in the future when these technologies will be more developed, the value of the current battery specific energy has been doubled to 500 Wh/kg.

6.3.1 Real range mission - 1150 km cruise

Study 1 - $C_{D0} = 0.0254$

For the first analysis the different analysed 8 missions will be compared against the baseline case results shown in table 6.3. The mission range and C_{D0} are fixed to the same values as the typical Cirrus SR-22 flight. The baseline cases for comparison will be calculated at an altitude of 3000 m for both cruise speeds.

On each column of table 6.4 the parameters selected are displayed. For columns 2 and 5 (h = 3000 m and E^*_{bat} = 250 Wh/kg) no parallel hybrid aircraft has been found to have a better performance than the conventional baseline aircraft, neither in terms of fuel consumption nor in MTOM or energy reduction. Therefore, these columns remain empty.

R = 1150 km C_{D0} = 0.0254	h = 3000 E^*_{bat} = 250 U = 90	h = 3000 E^*_{bat} = 500 U = 90	h = 1000 E^*_{bat} = 250 U = 90	h = 1000 E^*_{bat} = 500 U = 90	h = 3000 E^*_{bat} = 250 U = 75	h = 3000 E^*_{bat} = 500 U = 75	h = 1000 E^*_{bat} = 250 U = 75	h = 1000 E^*_{bat} = 500 U = 75
MTOM (kg)	-	1537.7	1591.6	1554.9	-	1283.2	1276.3	1237.4
W/S (N/m^2)	-	1324	1324	1324	-	1324	1324	1324
P/W (W/kg)	-	163.5	163.5	163.5	-	163.5	163.5	163.5
HP_{PH}	-	29.70%	28.10%	32.70%	-	54.10%	54.10%	57.20%
$HE_{average}$	-	1.57%	0.52%	0.60%	-	3.29%	1.20%	1.26%
Energy (MJ)	-	7903.3	8868.4	895.9	-	5075.5	5208	5222.5
m_{fuel} (kg)	-	194.5	218.8	221.4	-	124.3	128.2	128.6
m_{bat} (kg)	-	23.3	18	10.2	-	32.4	25.4	13
Conventional baseline aircraft at 3000 m altitude								
MTOM (kg)		1558.8				1308.5		
W/S (N/m^2)		1230				1010		
P/W (W/kg)		147.5				112.5		
Energy (MJ)		7691.8				5683.7		
m_{fuel} (kg)		190.1				140.5		
Relative change compared to conventional baseline aircraft								
MTOM (kg)	-	-1.35%	2.10%	-0.25%	-	-1.93%	-2.46%	-5.43%
W/S (N/m^2)	-	7.64%	7.64%	7.64%	-	31.09%	31.09%	31.09%
P/W (W/kg)	-	10.85%	10.85%	10.85%	-	45.33%	45.33%	45.33%
Energy (MJ)	-	2.75%	15.30%	-88.35%	-	-10.70%	-8.37%	-8.11%
m_{fuel} (kg)	-	2.31%	15.10%	16.47%	-	-11.53%	-8.75%	-8.47%

Table 6.4. Study 1 - Range = 1150 km, C_{D0} = 0.0254

Regarding the fast missions (U = 90 m/s) it can be observed how the ICE aircraft performs better even for the cases in which the battery specific energy has been doubled. Only for the second column a minor reduction about -1.35% for MTOM is achieved. The fuel mass and the energy consumed will increase for the three cases, meaning that there is no sense in applying a hybrid propulsion system if more fuel is going to be burned. This will go against the main objective of enabling hybrid propulsion, which is reducing fuel pollutant emissions to the atmosphere.

Since for high cruise speeds the HEA has not given a valuable solution to the fuel emissions reduction problem, it has been decided to decrease the cruise velocity. The new ICE baseline sized for this new speed shows a reduction of -16.04% in MTOM and of -26.5% in fuel mass, with respect to the high speed case. Taking a look at columns 6 to 9, slow cruise speed (U = 75 m/s), the parallel HEA shows a slight decrease in MTOM (no more than -5%) but a significant benefit on fuel mass reduction (between -8% and -10%). This is an important result, because it implies that if the propeller is not controlled by the high cruise speed restriction, less fuel will be required to propel the HEA aircraft. Accordingly, it can result profitable to apply a parallel hybrid configuration if the TLARs

are reduced, thus implying a lower performance that for the original TLARs.

As mentioned in section 6.2, the stall velocity constraint will limit the power profited from the batteries. As it can be seen on the table all the wing loading values are equal to the stall constraint limit $W/S_{max} = 1324$ N/m^2. Also, the results for high cruise speed show that the original Cirrus SR-22 was sized really close to its best design point for the ICE engine. This is why the HEA cannot offer any improvement in any of the analysed performances. As depicted in the constraint diagram of figure 5.2, the design point requires a precise trade-off between the three main constraints (Take-off, cruise and rate of climb).

Study 2 - $C_{D0} = 0.02$

This second study will be identical to the previous one with the only difference that the zero-lift drag coefficient has been reduced to 0.02. This can be related to a reduction in parasitic drag coming from the retraction of the landing gear and any high-lift devices or a new aircraft configuration which lowers the drag. The next table shows the corresponding results in the same way as the previous one. This time the ICE baseline aircraft must be recalculated for the new C_{D0}.

Again, the conventional design for fast cruise speed (U = 90m/s) outperforms the HEA. Nevertheless, if the battery technology is improved to a specific energy of 500 Wh/kg, there appear considerable reductions in fuel mass and energy used (about a -10%). Also, the MTOM is reduced a bit and the wing loading is increased to the stall speed limit.

Regarding the two cases at low altitude (h = 1000 m) and high cruise speed (U = 90 m/s), really few fuel savings are obtained. As it has been already discussed in previous chapters, implementing a hybrid propulsion system to an aircraft involves a high degree of complexity to the design and sizing process. Therefore, such a small benefit is not worth all the problems and resources spent in designing an aircraft mission like the ones of columns 4 and 5.

By reducing the cruise speed to 75 m/s, remarkably significant fuel savings are found. This time about a -20% of variation is achieved for energy and fuel mass. It can be observed how for low altitudes (1000 m) the benefits are even greater than for high altitudes. Furthermore, for future battery technologies the MTOM and fuel savings increase even more as it should be expected. As a result, these sets of parameters fit pretty well the HEA design concept and objective. However, it must be mentioned that the W/S stall limit has been reached again for the two last missions. This is traduced in a decrease of the profitability of the hybrid architecture, implying that a greater fuel reduction could be achieved if the stall speed constraint was increased. This will imply, see equation 5.12 to increase the maximum lift coefficient or to increase the stall speed which will lead to further aerodynamic design problems.

	h = 3000	h = 3000	h = 1000	h = 1000	h = 3000	h = 3000	h = 1000	h = 1000
R = 1150 km	E*_bat = 250	E*_bat = 500	E*_bat = 250	E*_bat = 500	E*_bat = 250	E*_bat = 500	E*_bat = 250	E*_bat = 500
CD0 = 0.02	U = 90	U = 90	U = 90	U = 90	U = 75	U = 75	U = 75	U = 75
MTOM (kg)	-	1346.5	1366.7	1327.9	1235.6	1186.9	1171.9	1134.4
W/S (N/m$\hat{2}$)	-	1324	1324	1324	990	1260	1324	1324
P/W (W/kg)	-	163.5	163.5	163.5	109.1	152.5	163.5	163.5
HP_PH	-	43.40%	43.40%	46.50%	18%	59%	63.30%	64.80%
HE_average	-	2.67%	0.97%	1.03%	1.23%	4.11%	1.68%	1.72%
Energy (MJ)	-	5558.8	6092.9	6095.5	4477.5	3984.6	3888.3	3840.4
m_fuel (kg)	-	136.4	150.2	150.2	110.2	97.3	95.6	94.4
m_batt (kg)	-	28.2	23.2	12.1	22.7	31.9	26.7	13.2
Conventional baseline aircraft at 3000 m altitude								
MTOM (kg)			1377.7				1254.2	
W/S (N/m$\hat{2}$)			1090				990	
P/W (W/kg)			125				110	
Energy (MJ)			6142.4				4882.2	
m_fuel (kg)			151.8				120.6	
Relative change compared to conventional baseline aircraft								
MTOM (kg)	-	-2.26%	-0.80%	-3.61%	-1.48%	-5.37%	-6.56%	-9.55%
W/S (N/m^2)	-	21.47%	21.47%	21.47%	0.00%	27.27%	33.74%	33.74%
P/W (W/kg)	-	30.80%	30.80%	30.80%	-0.82%	38.64%	48.64%	48.64%
Energy (MJ)	-	-9.50%	-0.81%	-0.76%	-8.29%	-18.39%	-20.36%	-21.34%
m_fuel (kg)	-	-10.14%	-1.05%	-1.05%	-8.62%	-19.32%	-20.73%	-21.72%

Table 6.5. Study 2 - Range = 1150 km, C_{D0} = 0.02

6.3.2 Short range mission - 575 km cruise

Now the same studies with the same variation of parameters will be performed but for a shorter mission range, half the previous one (575 km). This evaluation will allow to asses the influence of the flight range on the HEA performance.

Study 3 - $C_{D0} = 0.0254$

For the third study, the baseline aircraft is sized for the lower range (R = 575 km) and the high (U = 90 m/s) and low (U = 75 m/s) speeds.

R = 575 km CD0 = 0.0254	h = 3000 E*_bat = 250 U = 90	h = 3000 E*_bat = 500 U = 90	h = 1000 E*_bat = 250 U = 90	h = 1000 E*_bat = 500 U = 90	h = 3000 E*_bat = 250 U = 75	h = 3000 E*_bat = 500 U = 75	h = 1000 E*_bat = 250 U = 75	h = 1000 E*_bat = 500 U = 75
MTOM (kg)	-	-	1284.1	1258.4	-	1136.9	1118	1086.4
W/S (N/m^2)	-	-	1324	1324	-	1120	1310	1324
P/W (W/kg)	-	-	163.5	163.5	-	129.3	161.1	163.5
HP_PH	-	-	32.70%	32.70%	-	36%	58.10%	58.70%
HE_average	-	-	1.11%	1.11%	-	3.77%	2.30%	2.34%
Energy (MJ)	-	-	4102.7	4020.6	-	2915.1	2729	2625
m_fuel (kg)	-	-	101.1	99.1	-	71.3	67	64.4
m_batt (kg)	-	-	17	8.3	-	20.6	23.9	11.7
Conventional baseline aircraft at 3000 m altitude								
MTOM (kg)			1285.9			1148.9		
W/S (N/m$\hat{2}$)			1136			1010		
P/W (W/kg)			132.1			112.5		
Energy (MJ)			4216.5			2939.2		
m_fuel (kg)			104.2			72.6		
Relative change compared to conventional baseline aircraft								
MTOM (kg)	-	-	-0.14%	-2.14%	-	-1.04%	-2.69%	-5.44%
W/S (N/m$\hat{2}$)	-	-	16.55%	16.55%	-	10.89%	29.70%	31.09%
P/W (W/kg)	-	-	23.77%	23.77%	-	14.93%	43.20%	45.33%
Energy (MJ)	-	-	-2.70%	-4.65%	-	-0.82%	-7.15%	-10.69%
m_fuel (kg)	-	-	-2.98%	-4.89%	-	-1.79%	-7.71%	-11.29%

Table 6.6. Study 3 - Range 575 km $C_{D0} = 0.0254$

Similarly to the first study, the conventional ICE aircraft has demonstrated a better performance than HEA for high altitude (h = 3000 m), even for the improved battery technology. When the altitude is decreased to 1000 m, a small reduction in MTOM and fuel mass is achieved. However, this is too small (-3%) to call it a worthy benefit of

HEA. Just as it happened in previous cases, the wing loading is the one fixed by the stall constraint.

When the cruise speed is reduced to 75 m/s, a significant reduction in energy consumption and fuel (-30.3% for both) is achieved for the conventional aircraft, just as expected also in the rest of studies. Nevertheless, if the parallel hybrid configuration is implemented even a grater reduction is obtained. The results show a better performance again for the low altitude missions: -7.7% saving in fuel mass for the current battery technology and -11.3% reduction for the improved technology. From table 6.6 it can be concluded that the HEA shows a better performance than conventional aircraft for lower range flights.

It must be pointed out that this time the 8th column wing loading is below the stall limit, meaning that its full potential is being developed. On the other hand, for the 9th column (improved battery) the stall limit has been reached.

Study 4 - $C_{D0} = 0.02$

This final study aims to analyse the improvements obtained from the reduction of C_{D0}. As it should be expected from table 6.7's results, the fuel reduction benefits will be even greater for a lower drag coefficient.

	h = 3000	h = 3000	h = 1000	h = 1000	h = 3000	h = 3000	h = 1000	h = 1000
R = 575 km	E*_bat = 250	E*_bat = 500	E*_bat = 250	E*_bat = 500	E*_bat = 250	E*_bat = 500	E*_bat = 250	E*_bat = 500
CD0 = 0.02	U = 90	U = 90	U = 90	U = 90	U = 75	U = 75	U = 75	U = 75
MTOM (kg)	-	-	1174.4	1144.8	1116	1074.6	1058.2	1028.2
W/S (N/m$\hat{2}$)	-	-	1320	1324	990	990	1200	1280
P/W (W/kg)	-	-	162.8	163.5	109.1	109.1	142.3	155.9
HP_PH	-	-	46.30%	46.50%	18%	34%	59.60%	64.70%
HE_average	-	-	1.88%	1.89%	2.15%	3.96%	2.68%	3.01%
Energy (MJ)	-	-	3019.2	2932.6	2420	2448.7	2222.1	2073.6
m_fuel (kg)	-	-	74.2	72.1	59.4	59.9	54.5	50.8
m_batt (kg)	-	-	21.3	10.4	20.5	18.1	22.7	12
Conventional baseline aircraft at 3000 m altitude								
MTOM (kg)			1182.4			1119.4		
W/S (N/m^2)			1024			850		
P/W (W/kg)			114.2			107.5		
Energy (MJ)			3424.5			2673.8		
m_fuel (kg)			84.6			66.1		
Relative change compared to conventional baseline aircraft								
MTOM (kg)	-	-	-0.68%	-3.18%	-0.30%	-4.00%	-5.47%	-8.15%
W/S (N/m$\hat{2}$)	-	-	28.91%	29.30%	16.47%	16.47%	41.18%	50.59%
P/W (W/kg)	-	-	42.56%	43.17%	1.49%	1.49%	32.37%	45.02%
Energy (MJ)	-	-	-11.84%	-14.36%	-9.49%	-8.42%	-16.89%	-22.45%
m_fuel (kg)	-	-	-12.29%	-14.78%	-10.14%	-9.38%	-17.55%	-23.15%

Table 6.7. Study 4 - Range 575 km $C_{D0} = 0.02$

Just as happened in table 6.5, W/S and P/W are reduced for both type of aircraft. The obtained results show a greater fuel and energy saving from the comparison between the ICE aircraft and the HEA, this time of the order of -10% for slow and high altitude missions and -20% for slow and low altitude missions. For this study, the stall limit is only reached for the 5th column, meaning that the rest of missions are benefiting from its full potential.

6.3.3 Results conclusions

On this section, the most valuable results from the previous tables will be summarised and assessed. This has been decided to be done because of the large number of parameters that have been given in the previous sections.

Since in total 8x4 = 32 different flight parameter combinations have been evaluated all along this report, it is difficult to properly interpret the huge number of results obtained.

As a result, the following two graphs have been build to easily read the evolution of the fuel mass with the change in range and zero-lift drag coefficient.

It should be pointed out that only the cases corresponding to h = 1000 m have been compared since they were the only columns which gave meaningful data over the ICE baseline aircraft for the previous 4 studies. The legends of the graphs are written with the following nomenclature m_fuel (h-E^*_{bat}-U), like that it is possible to know the parameters used to obtain each value.

The graph below shows the evolution of the fuel mass difference with the conventional baseline aircraft for a constant C_{D0} = 0.0254 and the two evaluated ranges.

The tendency shows that for high cruise speeds (U = 90 m/s), a range reduction will imply passing from increasing the fuel mass to reducing the fuel mass when the hybrid system is implemented. Moreover, for slow speeds the effect of the range reduction is not that big. However, it can be clearly seen how for both ranges the speed reduction to 75 m/s gives a significant fuel mass saving compared with the fast cruise speed missions.

The most important conclusion to extract from here is that it is not worth to decrease the mission range and the cruise speed at the same time. It seems more logical to design a hybrid aircraft with a cruise speed a bit lower but which will cover the same range as the original one. Like that, almost the same performance is being provided by the HEA.

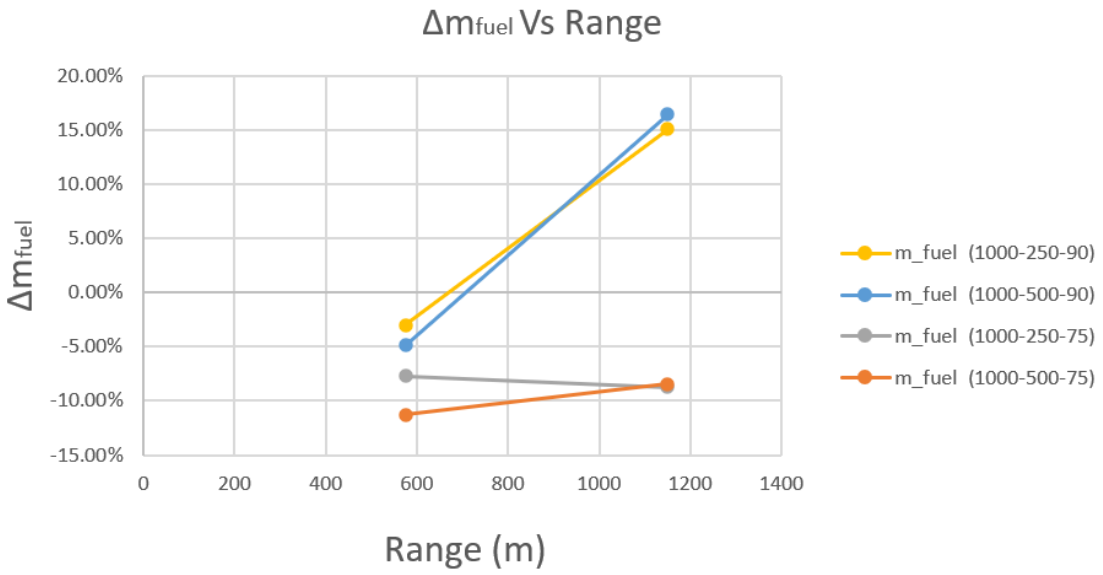

Figure 6.2. Fuel mass increment Vs Range

For this second graph, the real values of C_{D0} have not been displayed since the 0.0254 and 0.02 are two values really close and the lines will not be clearly displayed. Therefore C_{D0} = 0.02 is located in 0.5 and C_{D0} = 0.0254 is located in 2. The values displayed in the graph correspond to a constant range of 575 km.

As it was already mentioned, a reduction in C_{D0} will allow to save more fuel mass. This can be also inferred from the constraint equations 5.10 and 5.11. A decrease in C_{D0}

= $C_{D,min}$ will reduce the power loading and therefore the required energy and fuel mass for any chosen design split point.

Moreover, the trends show that when a higher battery specific energy is available the benefits in fuel savings are even greater. Also, the low speed missions show a better fuel reduction than the high speed missions. Obviously, it is more beneficial for the environment to fly at lower speeds but this may be a problem for airlines since the same distance will be covered in a larger time.

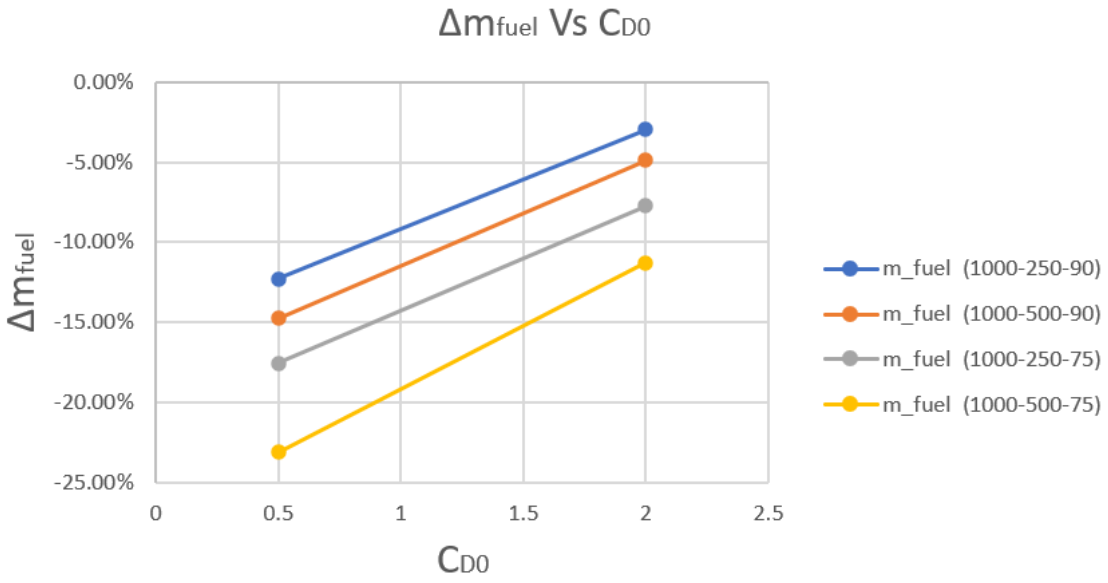

Figure 6.3. Fuel mass increment Vs C_{D0}

Another important result to be mentioned is that for every hybrid design the wing loading and the power-to-weight ratio have increased. This means that that the design point in the constraint diagram will be deviated to the right and up. As shown in figure 5.2 a design point up to the right will be completely given by the take-off distance constraint.

Furthermore, since the aspect ratio is kept constant during the sizing process; an increase in the W/S will decrease the wing area and therefore the wing span and the mean chord length (AR = b^2/S = b/c). This can be seen as a benefit if for example hangar space is a critical issue.

Now, the conclusions extracted from the 4 studies performed will be summed up:

- A decrease in the cruise speed will give fuel savings up to -8% for low altitudes and -10% for high altitudes technology, both for long mission range. If the drag coefficient is reduced to 0.02, this fuel savings are even greater (-20% to -21% depending on battery technology for low altitudes).
- An increase in the battery specific energy technology has proved to give substantial fuel savings for almost every mission configuration. For example at table 6.5 between columns 5 and 6 there is a change from -8.62% to -19.32%.

- A reduction in range will give greater fuel benefits for a higher cruise speed. This means that either the mission range or either the cruise speed should be decreased to extract a higher benefit from HEA, but not both at the same time. However, it has been determined more profitable from the economical point of view that a reduction in range is not worth since the aircraft will not be covering the same distance as the conventional original mission.

7 | Battery strategy

This chapter aims to present a battery strategy for the electric motor of the hybrid propulsion system to efficiently use the available electric energy during flight.

In the previous analysis, the ICE engine was supposed to operate at its optimum point during cruise. Therefore, the EM was only used in take-off, climb and landing phases. A direct result from this is that when the advanced technology batteries (500 Wh/kg) were used, the benefits on fuel and energy saving where not as high as it could be expected. Accordingly, if a battery strategy is designed to additionally use the battery in punctual moments of the cruise phase, greater benefits could be achieved.

7.1 Description of the analysis

The following study conducted by Julian Hoelzen [34] shows the benefits of implementing a battery energy strategy for the short range regional aircraft ATR-72. The aircraft data can be extracted from [35][36]. The new designed ATR-72 will be propelled by two electric driven wing tip propellers and a conventional gas turbine on each wing. The original aircraft is designed for 48 passengers, with a design range of 800 NM (1481.6 km) and a MTOM of 16150 kg.

The hybrid propulsion system will be in parallel because, as already seen in this report, it provides a lower weight and lower maintenance costs. The batteries chosen for the analysis will be Li-S with a gravimetric density of 650 Wh/kg, which is a bit optimistic for the current technology.

The objective of this analysis is just to show the improvements offered by the battery strategy implementation. Only the trends followed by the results will be analysed. Therefore, the numerical calculations will not be evaluated in depth as in the previous study.

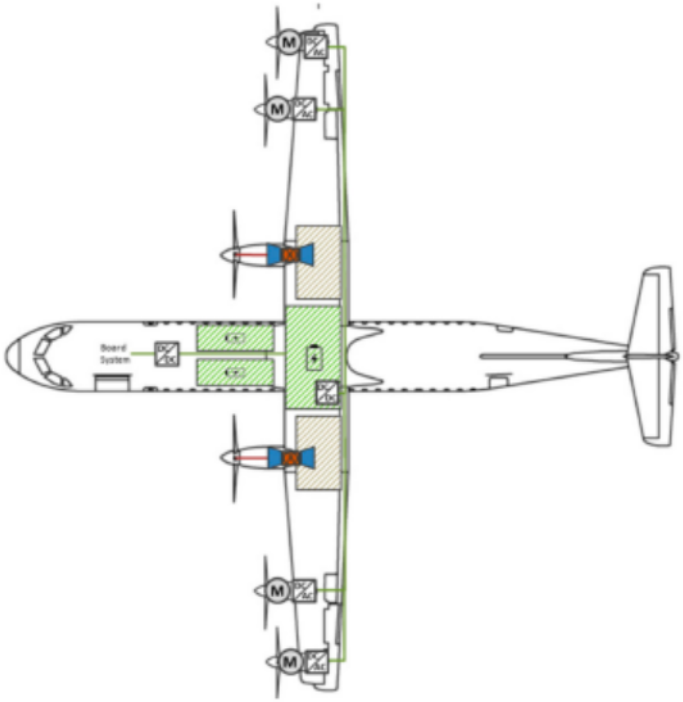

Figure 7.1. Hybrid architecture for ATR-72 [34]

7.2 Battery energy strategy

In the following figures a schematic graph of the source of energy used on each flight phase is shown. The phases considered are Taxi, take-off, climb, cruise, descent and landing. Originally, there exist two main methods of using the battery energy:

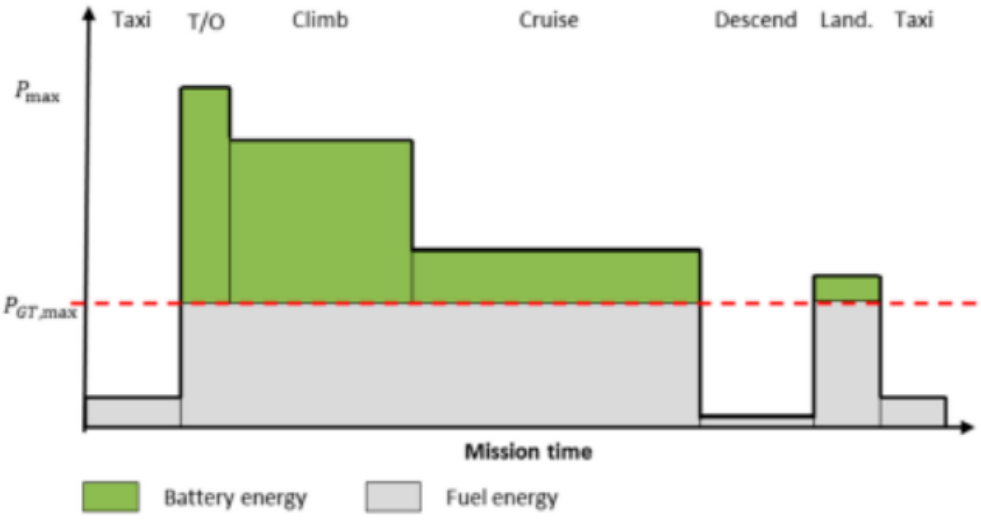

Figure 7.2. Maximum power peak shaving strategy

In figure 7.2 the battery is sized to the minimum required, it provides energy for **maximum power peak shaving** of the gas turbine power rating. If the gas turbine is not operating at its maximum power (red dashed line), the EM is not used. Like this, it is possible to downsize the ICE by adjusting the energy demand with the surplus of the EM.

For the analysis performed in chapter 6 the ICE was capable to provide all the power required for cruise phase on its own because it was sized to do so. Therefore the EM was only used for take-off and climb phases. Like this, the weight added by the batteries is reduced to the minimum, hence reducing MTOM as it was done in the previous chapter.

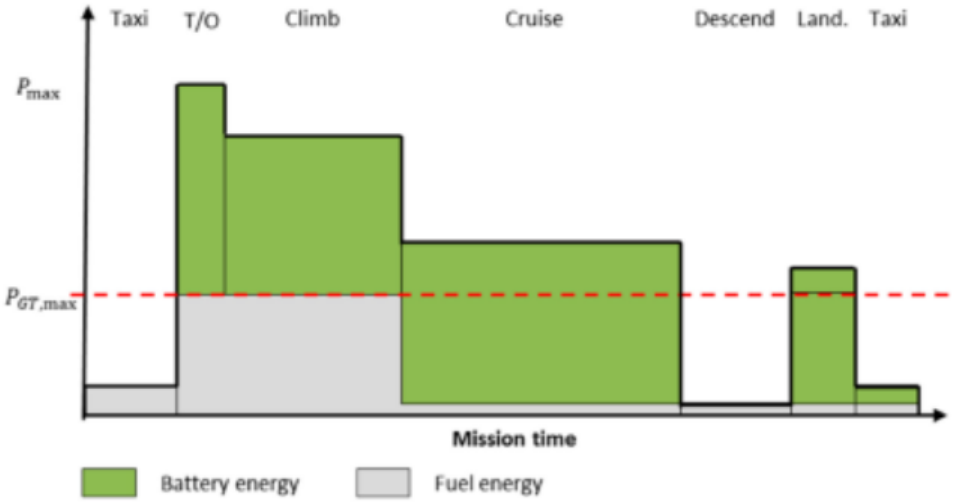

Figure 7.3. Maximum battery utilization strategy [34]

On the other hand, figure 7.3 shows the opposite point. This strategy tries to **consume the battery as much as possible**. As a result, the fuel mass required will be reduced in comparison with the previous strategy, but the MTOM will increase due to the batteries'weight. As already explained the energetic density of the batteries is lower than that of the fuel and the fuel is a consumable energy source.

This strategy is suitable for reducing CO_2 and any other greenhouse effect fuel emissions if the increase in MTOM is not a critical issue for the rest of the aircraft design. It is important to assess the impacts on the airframe structure of a greater MTOM, to see if the structure should be either reinforced or either reduce the payload.

After having analysed the two principal battery strategies, a new approach has been defined as the optimum solution in between these two extremes. The parameter λ_{bat} is defined ranging between [0, 1] to assess the battery energy employed. From the chosen degree of hybridization the required maximum power can be computed and the battery will be sized in accordance.

For this approach it has been assumed that batteries with low power densities could be oversized to meet certain energy capacity requirements. Provided that, it is highly beneficial to profit this energy oversizing without gaining any weight penalty. Consequently, a variable strategy as a function of λ_{bat} parameter is introduced for every DoH to test

different battery operation strategies between the two already defined approaches.

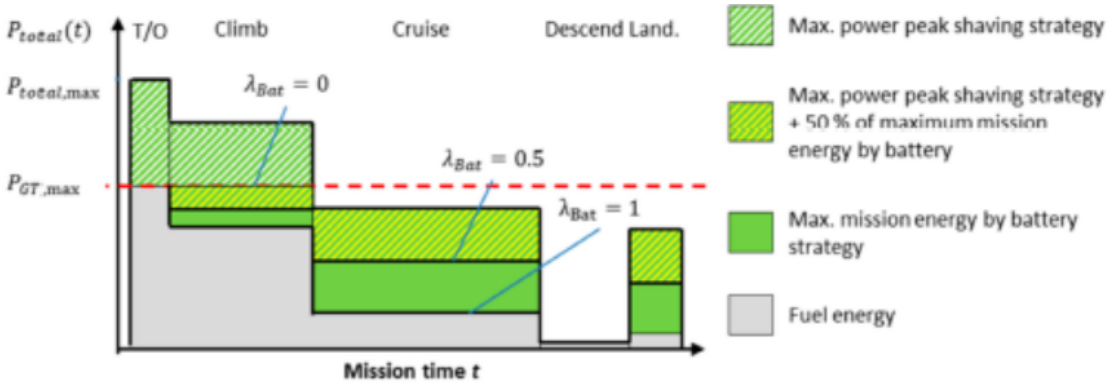

Figure 7.4. Battery strategy parameter definition [34]

The following equation defines the electric power as a function of the new battery strategy parameter.

$$P_{EM}(t) = max(P_T(t) - P_{ICE,max},\ 0) + \lambda_{bat} \cdot (min(P_{EM,max},\ P_T(t)) - max(P_T(t) - P_{ICE,max},\ 0)) \tag{7.1}$$

As depicted in figure 7.4, for every mission it is possible to define a new λ_{bat} parameter which provides the optimum trade-off between MTOM and required fuel mass without increasing the batteries weight that much. $\lambda_{bat} = 0$ will correspond to the maximum power peak shaving strategy defined in figure 7.2 and $\lambda_{bat} = 1$ to the maximum battery utilization strategy showed in figure 7.3.

7.3 Results of the study

The following graphs show the simulation results performed by the software used in [34] for ATR-72 aircraft. The results show the power degree of hybridization H_P = [0.1, 0.9] and in the X-axis and the λ_{bat} strategy parameter in the Y-axis. The colour map will cover the range of values for the battery mass and the battery usage.

The study of these results is only intended to prove that even a greater fuel mass reduction could be obtained from the previous analysis. However, the battery strategy parameter should be carefully implemented to the already defined sizing methodology and its equations.

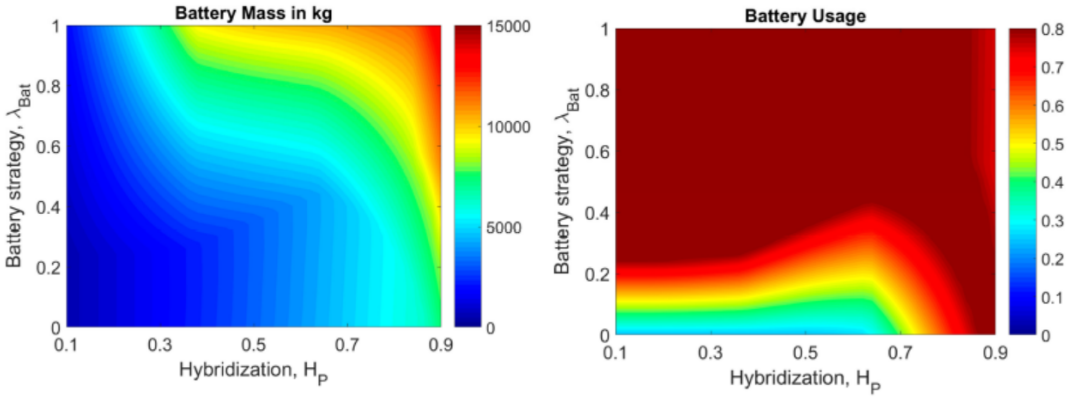

(a) Battery mass Vs H_P and λ_{bat}

(b) Battery usage Vs H_P and λ_{bat}

Figure 7.5. Battery mass and usage [34]

From figure 7.5a it can be checked that the higher H_P, the greater the battery mass. However, the weight growth relation is not linear. It can be observed a great increase in battery mass for $H_P > 0.8$. Now if we look at the battery strategy parameter, for every λ_{bat} there is a specific H_P that will minimize the battery weight. For example, $\lambda_{bat} = 0.3$ with $H_P = 0.4$. It must be mentioned that is not always true that the higher the H_P and λ_{bat}, the more fuel will be saved. This is only true as long as the battery mass does not grow considerably.

It can also be observed how for high battery strategy parameters (over 0.65 - 0.7) higher battery masses are found even for low $H_P < 0.4$. On the other hand, for moderate $\lambda_{bat} < 0.6$ an appropriate battery weight below 8000 kg is found approximately for $H_P < 0.9$.

The second figure shows the battery usage percentage. Its maximum is set to 0.8 since the depth of discharge of the battery is of 20%. The following colour map shows the exploitation of the battery energy, which is sized according to energy requirements or maximum power output. As explained before, the battery is better exploited for higher λ_{bat} since more battery energy is being profited for the same H_P.

From figure 7.5b it can be observed that for a fixed $\lambda_{bat} = 0.2$ battery usage first decreases between H_P [0.1, 0.6] and then it starts to increase for $H_P > 0.6$. This is explained because for low hybridization, the power rating increases significantly more than the energy demand. Only for the phases in which a peak power is required such as take-off and climb, which last no more than 20 minutes, are substituted with the electric propulsion system. Consequently, the power and not the energy demand increases significantly.

The opposite happens for higher hybridization degrees with the cruise phase. Since the cruise flight accounts for the longest part of the flight, a major demand of mission energy is required in this interval. Therefore, if the ICE is not sized to provide all the power for the cruise constraint as in the previous chapter, the battery usage will increase considerably to support the cruise phase.

Finally, it can be stated that the optimum trade-off combination is obtained for H_P

= 0.7 and λ_{bat} [0.5, 0.6] for which a battery mass about 5000 kg is required. As it is observed, the battery weight for such a H_P is the same for λ_{bat}= 0 than for 0.6. There are several vertical lines in the color map showing that weight does not change. However, the optimal mass for each H_P will depend on the full exploitation of the batter. On the second graph it can be seen how battery usage is at its maximum. It is not worth to carry a battery which is not going to be fully used, since the battery mass is always fixed. This is why we are trying to oversize the battery and extract the maximum possible profit from it.

Now, this study will be related with the one performed in chapter 6. The previous study considerations match with the definition of $\lambda_{bat} = 0$ (Maximum power peak shaving strategy) as it was performed with regards of minimising the MTOM and not the fuel mass required or the energy consumption. Therefore, applying a higher λ_{bat} parameter like 0.4 - 0.5 will allow to obtain a higher performance without increasing the battery mass and the MTOM as a consequence. It is also important to note that in chapter 6, for Cirrus SR-22, the cruise phase is completely covered by the ICE. As a result, the benefits from this battery strategy will not be as high as in ATR-72 study. Nevertheless, further investigation should be performed to adequately incorporate the concept of battery strategy parameter to the developed hybrid aircraft sizing algorithm.

8 | Conclusion

This report has analysed the main solution for reducing fuel consumption and pollutant emissions in the aviation sector: hybrid electric aircraft. After a review over its main architectures, it has been determined that for medium and small sized regional aircraft the parallel configuration will benefit from a simpler and lighter propulsion system.

Next, a state-of the art on the current and future battery technologies has been assessed. This study has shown that for the moment there is a big limitation for implementing FEA since the specific energy of a battery is about 250 Wh/kg. However, in the future this value is expected to reach 500 or even 750 Wh/kg for Li-Ion batteries.

The conventional sizing process for aircraft has been briefly explained. After this, a new methodology is presented for HEA. Its basis relies on the point performance analysis thanks to the constraint equations for take-off distance, cruise, climb and stall; and the mission performance. This second part of the scheme showed in figure 5.1 requires an iterative process for finding a MTOM which matches the requirements given by TLARs and the constraint diagram.

The calculations performed for Cirrus SR-22 present some interesting HEA designs. If the same mission (range, speed and altitude) is intended for a HEA, no potential fuel savings are observed. However, for lower speeds than the conventional cruise speed and for lower mission range, fuel reductions over -8% or -17% (depending on C_{D0}) can be achieved with the current battery technology. As a result, it is possible to reduce to a certain extent the fuel required for business and regional flights of 1150 km or less. As mission length is reduced, the power required decreases and therefore the battery weight.

Regarding the use of the batteries, hybrid-electric propulsion systems are best suited for aircraft with fluctuating power requirements. The best performance is achieved when combustion engines provide a constant power load and the extra needs of power are covered by the EM. This optimization will either result in an aircraft with a reduced MTOM, or an aircraft with reduced energy consumption, depending on the optimization objective. On this case the sizing process has been performed with the focus on minimising the MTOM. Also, the ICE was completely capable of providing all the required power for cruise.

Nevertheless, these results can be further improved if an optimum battery strategy is implemented. Until now, the battery was sized to reduce the MTOM as much as possible. Accordingly, the fuel mass reduction was not the best that could be achieved. In the last chapter, the battery strategy parameter λ_{bat} has been introduced. This relies on the

assumption that batteries with a low power, not energy, densities can be oversized without increasing the battery weight. For every degree of hybridization there exists an optimum λ_{bat} which will provide the best trade-off between MTOM and fuel reduction. A study based on ATR-72 aircraft has been analysed, proving that for H_P=0.7 a λ_{bat} about 0.6 will not increase the battery weight at all.

In overall, this report has proved the validity of hybrid aircraft designs for reducing the fuel burned during regional flights as an alternative to FEA. However, the current battery technology is a constraint which make HEA incapable of being fully competitive with ICE aircraft for the same TLARs. Nevertheless, it is possible to have substantial fuel savings if the aircraft performance is lowered in some aspects such as cruise speed or altitude. In the near future batteries will be improved and there will arrive the moment in which hybrid aircraft will become economical profitable for its commercialisation and industrialization.

Bibliography

[1] NASA aeronautics research mission directorate. Strategic implementation plan. Available at https://www.hq.nasa.gov/office/aero/pdf/armd-strategic-implementation-plan.pdf, June 2021.

[2] Europe. 2050-europe's vision for aviation. Available at https://ec.europa.eu/transport/sites/default/files/modes/air/doc/flightpath2050.pdf, June 2021.

[3] Safran. Hybrid electric propulsion - how it works. Available at https://www.safran-group.com/hybrid-electric-propulsion-how-it-works, February 2021.

[4] Paul Robertson. Hybrid power in light aircraft: Design considerations and experiences of first flight. Available at https://www.aerosociety.com/media/5962/3-hybrid-power-in-light-aircraft.pdf, October 2020.

[5] Tec.ieee.org. Hybrid electric aircraft: State of the art and key electrical system challenges - ieee transportation electrification community. Available at https://tec.ieee.org/newsletter/september-2016/hybrid-electric-aircraft-state-of-the-art-and-key-electrical-system-challenges February 2021.

[6] ICAO. Electric, hybrid, and hydrogen aircraft – state of play. Available at https://www.icao.int/environmental-protection/Documents/EnvironmentalReports/2019/ENVReport2019_pg124-130.pdf, October 2020.

[7] Wings Magazine. Rolls-royce advances hybrid-electric tests. Available at https://www.wingsmagazine.com/rolls-royce-advances-hybrid-electric-tests/, February 2021.

[8] Zhang PDAN Ye XIE, Tsourdos ANTONIOS and GU Jason. Review of hybrid electric powered aircraft, its conceptual design and energy management methodologies. Available at https://reader.elsevier.com/reader/sd/pii/S1000936120303368?token=23217F2BCA3EA0685646803D08E9C976F8F07CA9DA38F50592DDBB0F70D0515B1B9FB2B04AA2C27 February 2021.

[9] Diego Benegas Jayme. Evaluation of the hybrid-electric aircraft project airbus e-fan x. master thesis. Available at https://www.fzt.haw-hamburg.de/pers/Scholz/arbeiten/TextBenegasJayme.pdf, June 2021.

[10] Joris Van Bogaert. Assessment of potential fuel saving benefits of hybrid-electric regional aircraft. Available at https://repository.tudelft.nl/islandora/object/uuid%3A0fc7019f-d988-45c1-a7e2-55825f4f90ca, June 2021.

[11] Wikipedia. Available at https://en.wikipedia.org/wiki/Airbus_E-Fan, June 2021.

[12] Sarah J. Gerssen-Gondelach and André P.C. Faaij. Available at https://doi.org/10.1016/j.jpowsour.2012.03.085, June 2021.

[13] Mark Crittenden. Available at https://ieeexplore.ieee.org/document/9173903, June 2021.

[14] Kaushik Rajashekara. Available at https://ieeexplore.ieee.org/document/6507304, June 2021.

[15] Jan van Toor y Hans Lobentanzer Stefan Stückl. Available at https://www.icas.org/ICAS_ARCHIVE/ICAS2012/PAPERS/521.PDF, June 2021.

[16] Marcia Wade Talbert. Available at http://www.rexresearch.com/johnsonliairbatty/johnsonlibattery.htm, June 2021.

[17] Marty K Bradley y Christopher K Droney. Subsonic ultra green aircraft research phaseii: N+4 advanced concept development. Available at https://ntrs.nasa.gov/api/citations/20120009038/downloads/20120009038.pdf, June 2021.

[18] J; Gangoli Rao Arvind Voskuijl Mark; van Bogaert. Analysis and design of hybrid electric regional turboprop aircraft. Available at https://research.tudelft.nl/en/publications/analysis-and-design-of-hybrid-electric-regional-turboprop-aircraf, June 2021.

[19] uenergyhub.com. Available at https://i1.wp.com/uenergyhub.com/wp-content/uploads/2020/05/Universal-Ragone-3.png?fit=1097%2C820&ssl=1, June 2021.

[20] William H. Mason. Modern aircraft design techniques. Available at https://citeseerx.ist.psu.edu/viewdoc/download?doi=10.1.1.536.6188&rep=rep1&type=pdf, June 2021.

[21] SC Jensen. Role of figures of merit in design optimization and technology assessment. Available at https://doi.org/10.2514/3.57468, June 2021.

[22] Carsten Braun D. Felix Finger and Cees Bil. An initial sizing methodology for hybrid-electric light aircraft. Available at https://doi.org/10.2514/6.2018-4229, April 2021.

[23] Sabrina Corpino Luca Boggero, Marco Fioriti. Development of a new conceptual design methodology for parallel hybrid aircraft. Available at https://doi.org/10.1177/0954410017745569, April 2021.

[24] N. Rabizadeh and B Kasbi. Conceptual design of a transport aircraft. Available at https://www.semanticscholar.org/paper/Conceptual-Design-of-a-Transport-Aircraft-Rabizadeh-Kasbi/69ce11e9f3e796e4bb721edc508095a4711e5e99, April 2021.

[25] D. P. Raymer. Aircraft design: A conceptual approach. 6th ed. Available at https://soaneemrana.org/onewebmedia/AIRCRAFT%20DESIGN%20;%20A%20Conceptual%20Approach%20BY%20DANIEL%20P%20RAYMER.pdf, April 2021.

[26] L. M. Nicolai and G. E. Carichner. Fundamentals of aircraft and airship design. volume i - aircraft design. Available at https://doi.org/10.1017/S0001924000005388, April 2021.

[27] S. Gudmundsson. General aviation aircraft design: Applied methods and procedures. Oxford: Butterworth-Heinemann, 2014.

[28] Aviation Stack Exchange. What is the propeller efficiency, μ_p , of modern propellers for light sport aircraft? Available at https://aviation.stackexchange.com/questions/14305/what-is-the-propeller-efficiency-%CE%BC-p-of-modern-propellers-for-light-sport-ai, June 2021.

[29] Wikipedia. Available at https://en.wikipedia.org/wiki/Propeller_(aeronautics), June 2021.

[30] Carsten Braun D. Felix Finger and Cees Bil. Case studies in initial sizing for hybrid-electric general aviation aircraft. Available at https://doi.org/10.2514/6.2018-5005, June 2021.

[31] M. D. Moore M. D. Patterson, Brian J. German. Performance analysis and design of on-demand electric aircraft concepts. Available at https://doi.org/10.2514/6.2012-5474, June 2021.

[32] flyingmag.com. 2001 cirrus sr22. Available at https://www.flyingmag.com/pilot-reports/pistons/cirrus-sr22/, June 2021.

[33] Cirrus aircraft. Available at https://cirrusaircraft.com/aircraft/sr22/, June 2021.

[34] Boris Bensmann Julian Hoelzen, Yaolong Liu and more. Conceptual design of operation strategies for hybrid electric aircraft. Available at https://www.google.fr/url?sa=t&rct=j&q=&esrc=s&source=web&cd=&ved=2ahUKEwjIl_al2Z3sAhUuxoUKHb4GCZEQFjAEegQIBhAC&url=https%3A%2F%2Fwww.mdpi.com%2F1996-1073%2F11%2F1%2F217%2Fpdf&usg=AOvVaw2Ebz9ZeK2ul7JQANHgaUnZ, October 2020.

[35] ATR. Available at https://www.atr-aircraft.com/our-aircraft/atr-72-600/, June 2021.

[36] ATR. Available at https://1tr779ud5r1jjgc938wedppw-wpengine.netdna-ssl.com/wp-content/uploads/2020/07/Factsheets_-_ATR_72-600.pdf, June 2021.